Norwegian University
of Life Sciences

Master's Thesis 2024 60 ECTS
Faculty of Chemistry, Biotechnology and Food Science

Use of microcosm experiments to investigate the genetic potential for methylotrophic methanogenesis in marine sediments

Kari Anette Thomassen Hovind
Master of Science in Biotechnology

Summary

Wastewater treatment plants often use methanol to drive denitrification for nitrogen removal. This can lead to excess methanol reaching water bodies through the effluent discharge. This excess methanol can stimulate methylotrophic methanogenesis in marine sediments, potentially increasing methane production.

The current thesis investigated the enrichment of microorganisms capable of methylotrophic methanogenesis in sediment samples from the Oslo fjord. Microcosms consisting of sediment material and synthetic seawater were enriched in four different ways. Enrichments were performed using methanol, nitrate and methanol and nitrate together as well as a control. The microcosms were monitored over time by measuring NO_3^-, NO_2^-, NH_3/NH_4^+, pH and ORP every 2-3 days. Sediment samples were collected every 3-4 days and DNA was extracted. The extracted DNA was analysed using qPCR, 16S rRNA amplicon sequencing and shotgun metagenomic sequencing to investigate the inferred taxonomic composition and the genetic potential of the methylotrophic methanogens in the sediments.

The results revealed a significant enrichment of methanogenic archaea within the family *Methanosarcinaceae* for samples amended with methanol after 17 and 21 days of incubation at ORPs higher than +50 mV. This was both observed using relative read counts from 16S rRNA amplicon analysis, as well as FAPROTAX analysis that inferred metabolic processes to the taxa identified from the 16S rRNA sequences.

Investigation of the shotgun sequencing data revealed three MAGs that were taxonomically annotated as archaea belonging to the family *Methanosarcinaceae*. The genomic potential in each of these MAGs were investigated for presence of methanogenesis genes, and for completeness of the relevant pathways. Methyl reduction was revealed as the most probable methylotrophic pathway. The number of genes in each MAG that were related to methanogenesis from methanol varied, but all MAGs contained the genes mcrABG, mtaB and mtaC which convert methanol into methyl-CoM and further into methane. MtaA was identified in two of the three MAGs.

The enrichment of *Methanosarcinaceae* occurred at higher ORP measurements than expected from literature. This is an interesting aspect of the results, that should be followed up in future research based on methylotrophic methanogenesis in marine sediments.

Sammendrag

Moderne avløpsrenseanlegg bruker ofte metanol for å drive denitrifisering for å fjerne nitrogen. Dette kan føre til at overflødig metanol når vannforekomster når renset avløpsvann slippes ut av renseanleggene. Denne metanolen kan stimulere metylotrof metanogenese i sedimenter, noe som potensielt kan øke produksjonen av metan.

Denne masteroppgaven undersøkte anrikning av mikroorganismer i stand til å gjøre metylotrof metanogenese i sedimentprøver fra Oslofjorden. Mikrokosmer bestående av sedimentmateriale og syntetisk sjøvann ble anriket på fire ulike måter. Anrikningen ble utført med metanol, nitrat, metanol og nitrat sammen, i tillegg til en kontroll. Mikrokosmene ble overvåket over tid ved å måle NO_3^-, NO_2^-, NH_3/NH_4^+, pH og ORP hver 2-3 dag. Sedimentprøver ble tatt hver 3-4 dag, og DNA ble ekstrahert fra prøvene. Det ekstraherte DNA-et ble analysert ved bruk av qPCR, 16S rRNA amplicon-sekvensering og shotgun metagenomsekvensering for å undersøke den taksonomiske sammensetningen og det genetiske potensialet til de metylotrofe metanogene mikrobene i sedimentene.

Resultatene avslørte en signifikant anrikning av metanogene arker tilhørende familien *Methanosarcinaceae* for prøver som ble anriket med metanol, etter inkubering i 17 og 21 dager ved ORP-målinger høyere enn +50 mV. Dette ble observert både ved bruk av relative readcounts fra 16S rRNA-ampliconanalysen, i tillegg til FAPROTAX-analysen som antydet metabolske prosesser innad i de taksonomiske gruppene identifisert fra 16S rRNA-sekvensene.

Tre MAGs ble taksonomisk klassifisert som arker tilhørende familien *Methanosarcinaceae* etter gjennomført assemblering av shotgun-sekvenseringen. Det genetiske potensialet i hver MAG ble undersøkt for metanogenese-gener, og for hvor fullstendige de ulike potensielle metabolske stiene var. Metyl-reduksjon ble detektert som den mest sannsynlige metylotrofe stien. Antallet gener i hver MAG som var relevant for metanogenese fra metanol varierte, men alle MAGsene inneholdt genene mcrABG, mtaB og mtaC som omdanner metanol til metyl-CoM og videre til metangass. MtaA ble identifisert i to av tre MAGer.

Anrikningen av *Methanosarcinaceae* ble observert ved høyere ORP enn forventet basert på informasjon fra litteraturen. Dette er et veldig interessant aspekt av resultatene som bør følges opp i fremtidige forsøk som omhandler metylotrof metanogenese i marine sedimenter.

Acknowledgements

The work in this thesis was carried out at the Faculty of Chemistry, Biotechnology and Food Sciences, at the Norwegian University of Life Sciences, under the supervision of Professor Knut Rudi and Professor Lars Snipen. I am very grateful for the opportunity to write this thesis under your supervision, and for your support and guidance the past year.

I would also like to extend my thanks to Morten, Karen, Tonje, Ida, Inga, Melcy, Jenny, Else and Fiona for immeasurably valuable help and guidance in the lab, and for always meeting me with a smile.

I would not have been able to do this without the company of my fellow master student Kathrine. I have enjoyed immeasurably to be in the lab together with you. I don't know where I would have been right now without your company. And also thank you Ragnhild for the company in the lab in December when we both were doing things we had not done before, but at least we did it together.

I extend an extra thanks to Julie for her incredibly valuable help and support. Without you this would have been a much lonelier process, and I wouldn't have known half the things I know now. Thank you for answering all my stupid questions, motivating me and being so supportive in the challenge this has been.

And lastly, thank you to my friends, family and boyfriend that have supported me throughout all the work this has been. For always listening and understanding and helping me when I needed it.

Kari Anette Hovind

May, 2024

Abbreviations

16S rRNA – A gene encoding the small subunit of microbial ribosomes. It contains hypervariable regions that can be used for taxonomic annotation of bacterial and archaeal cells.

Bin – Several reads and/or contigs belonging to an individual genome

BOD – Biological oxygen demand

COD – Chemical oxygen demand

Contig – A longer sequence of bases assembled from reads.

Cq – The cycle threshold from a qPCR run. This value represents at which cycle in the qPCR-run the DNA concentration surpasses the fluorescence threshold.

DIC – Dissolved inorganic carbon

DNRA – Dissimilatory nitrate reduction to ammonium

DOC - Dissolved organic carbon

In situ – "on site", meaning experiments done in their natural environments

MAG – Metagenome assembled genome

N_0 – A baseline corrected Cq value. Provides an estimating starting concentration of DNA in the sample, expressed in relative fluorescence units (RFUs)

ORF – Open reading frame

ORP – Oxidation reduction potential

OTU – Operational Taxonomic Unit

PCoA – Principal Coordinate analysis

PCR – Polymerase chain reaction

qPCR – Quantitative polymerase chain reaction

Disclaimer: The use of AI in this thesis

Artificial intelligence has been used as an aid in the writing of this thesis. It was used to assist with scientific writing and alternative phrasing. AI was not used for coding during the data analysis of the thesis.

1 Introduction

More than 70% of the globe is covered by water. The oceans, that make up the majority of the water bodies, are home to a plethora of species that share this vast ecosystem. Marine microbiological life represent approximately 50% of the world's primary production and is therefore immeasurably valuable for both life on land and in the oceans (Chavez et al., 2011). Over the last century, anthropogenic impact on marine environments have increased. Climate change have had detrimental effects on marine ecosystems and is thought to be a leading cause to loss of biodiversity in the oceans (Gruber et al., 2021). Increasing our well of knowledge can help us learn what measures will be effective for promoting sustainability and reducing anthropogenic impacts on marine food networks.

1.1 Marine ecosystems are under pressure

Marine food chains are long and complex and are often longer than their terrestrial counterparts. This indicates that nutrients have to be transported through more trophic levels to get to the top of the food chain (McGarvey et al., 2016). Because aquatic networks have many trophic links, imbalances can easier occur, and even small impacts can have large consequences. The oceans harbour organisms that form a cycle of production, degradation, and recycling of all compounds necessary for sustaining life (Landrigan et al., 2020).

Even though nutrients are being recycled in the oceans, there are limiting factors. The limiting nutrient in marine ecosystems is usually either nitrogen and/or phosphorous (Oviatt et al., 1995). In recent years, there has been a net increase of nitrogen input to benthic environments, due to activities such as agriculture and industry (Galloway et al., 1995). This could in turn affect aquatic environments and organisms such as marine primary producers (Hallegraeff, 1993).

Increased availability of nitrogen can lead to algal blooms. The formation of algal mats can reduce the penetration of sunlight to deeper depths of waters which can inhibit the growth of other photosynthetic species dependent on sunlight. When the algae die, they sediment and become a source of carbon for heterotrophic microorganisms in deeper layers of the water. Increased heterotrophic activity can lead to oxygen depletion in the water column, which can cause death of marine life (Hallegraeff, 1993).

Oceanic environments are under pressure from several anthropogenic activities. Runoff from agriculture, the use of fossil fuels in waterborne vehicles, and the disposal of wastewater are some sources of pollution. Ocean warming, acidification, and deoxygenation are often

considered the main threats to marine ecosystems (Gao et al., 2012). In recent years there has been an increasing focus on reducing emissions of especially nitrogen species. One measure that has been implemented is the purification of wastewater from households and industry.

1.2 Wastewater treatment

Before wastewater treatment plants were taken in use, raw sewage was released straight into nature. It contained significant amounts of excess carbon and nitrogen and greatly contributed to eutrophication of areas where the wastewater was released (Akinnawo, 2023).

The first wastewater treatment facility in Oslo was completed in 1910. This was a purely mechanical treatment plant which could remove about one fifth of the undissolved substances in the wastewater. In 1931 the first activated sludge facility was constructed. In the following years, large sums were invested in the wastewater treatment in Oslo, but the municipality struggled to keep up with the growing population. In the 1950's, researchers at Oslo University observed that the depths of Bunnefjorden were practically anoxic due to eutrophication from wastewater. From then on, more wastewater treatment facilities were built, and wastewater treatment has since become an unavoidable feature of society (Johansen, 2001).

Modern wastewater treatment plants utilise a combination of physical, chemical, and biological processes to purify wastewater. These processes are usually divided into three different stages, primary, secondary, and tertiary treatment. Primary treatment consists of removing debris, suspended solids and some dissolved carbon through filtration and sedimentation. Secondary treatment involves the oxidation of dissolved carbon (DIC; dissolved inorganic carbon and DOC; dissolved organic carbon) and other solutes using chemical and physical methods. Biological degradation can also be a part of the secondary treatment. Lastly, a tertiary purification step is included in certain treatment plants. It involves biological or chemical treatments to remove elements such as phosphorous and nitrogen. Tertiary treatment often utilise biological processes carried out by specific microbes to achieve necessary purification (Sonune & Ghate, 2004).

Biological nitrogen removal is based on two microbial metabolic processes: nitrification, and denitrification (Thakur & Medhi, 2019). Nitrification is an aerobic process where ammonia (NH_3) is oxidized to nitrate (NO_3^-) by chemolithoautotrophic organisms. Denitrification is the anaerobic reduction of nitrate to N_2-gas through a series of reduction steps (Hutchins & Capone, 2022). Due to the preliminary treatment steps, there is a lack of carbon in the water and since denitrification is a heterotrophic process, an external carbon source is added. This is supplied

in form of a small molecular weight carbon compound – often methanol. Methanol is used as it is the cheapest option for a carbon-supplement for the denitrifying bacteria (Gan et al., 2023). To efficiently reduce nitrogen species such as ammonia and nitrate to nitrogen gas, a surplus of carbon is needed. The C/N ratio utilised will vary between treatment plants (Mishra et al., 2022; Nyberg et al., 1992; Pelaz et al., 2018).

1.2.1 Wastewater treatment plants in Norway

There are four densely populated areas in Norway that have requirements to remove a minimum of 70% of the nitrogen in the wastewater. These areas are Nordre Follo, Oslo, Jessheim, and Lillehammer (Forurensningsforskriften, 2004). Several treatment plants within these areas will release their effluent water into the inner Oslo fjord, which is an area under constant surveillance because of its vulnerability to anthropogenic activities.

The Oslo fjord is separated into two water bodies: the inner and outer fjord. The separation goes at Drøbaksundet, a narrow and shallow part of the fjord. Figure 1.1 marks this division with a red line. Because of the geographic confinement of the inner Oslo fjord, there is reduced replacement of the water masses, which makes the accumulative effects of pollution in this area even bigger (SALT, 2019). To reduce the burden on the inner Oslo fjord, several wastewater treatment facilities in this area utilise tertiary wastewater treatment (Forurensningsforskriften, 2004). In figure 1.1 their location is marked with red dots.

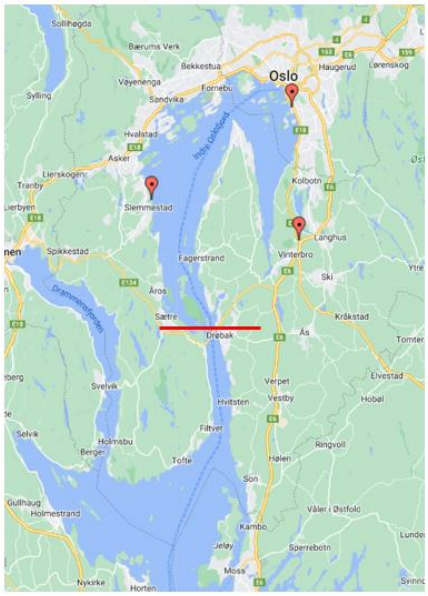

Figure 1.1: The Oslo fjord, marked with the three wastewater treatment facilities that use biological nitrogen removal, as well as the separation between the inner and outer fjord. The figure was made with ZeeMaps (https://www.zeemaps.com/).

In the past decades, there has been a growing awareness of the environmental impact of nitrogen in eutrophication processes (de Vries, 2021). Consequently, governments are increasing their regulations concerning nitrogen removal from wastewater. As more treatment plants implement biological nitrogen removal, there will also be a potential increased use of organic carbon to support denitrification.

The Norwegian government has established regulations regarding wastewater purification. Most regulations are concerning biological oxygen demand (BOD) and chemical oxygen demand (COD). BOD_5 is the amount of oxygen used by microorganisms over 5 days, measured in mg O_2/L. COD is the amount of oxygen needed for complete oxidation of all organic carbon compounds into CO_2 and water (Aguilar-

Torrejón et al., 2023). Primary treatment should reduce BOD_5 by at least 20 % or to no more than 40 mg O_2/L, as well as reduce the suspended solids to no more than 60 mg/L. Plants with tertiary treatments, need to reduce BOD_5 to 25 mg O_2/L and COD to no more than 25 mg O_2/L. Additionally, tertiary treatment plants must adhere to regulations regarding how much nitrogen and phosphorous should be removed (Forurensningsforskriften, 2004).

Apart from BOD_5 and COD there are no direct regulations as to how much and what types of organic carbon there can be in the effluent wastewater (Forurensningsforskriften, 2004). We lack information on whether the effluent water has a significant content of organic carbon, and what compounds it is comprised of.

1.3 Organic compounds

Organic carbon is an essential component in nutrient cycling and energy production in various environments (Amon & Benner, 1996). Organic compounds are defined as compounds that contain carbon (Bruice, 2016). Organic compounds are interesting because carbon is an atom that shares electrons. It seldom gives up or receives them, but shares them with other atoms, forming covalent bonds. This unique property of carbon enables the formation of stable compounds with a broad spectrum of chemical properties.

The simpler organic molecules are the alkanes. They are hydrocarbons bonded either linearly, circularly or branched, and are stable and chemically inert (Rojo, 2009). Another group of stable, but less inert compounds are the methyl compounds. They are smaller than most alkanes, and they do not have the carbon-carbon bonds that all alkanes (except methane) have. Methyl compounds can be degraded by methylotrophic organisms. Methylotrophic organisms must synthesize all carbon-carbon bonds for cellular processes themselves. Organisms that use more complex organic compounds as a substrate can avoid this to some extent (Anthony, 1975).

1.3.1 Methyl compounds

Within organic chemistry, methyl-compounds have simple structures, but they can contain nitrogen, oxygen, or other elements (Anthony, 1975). Some of the more common methyl-compounds are listed in table 1.1.

Table 1.1: Overview of some common methyl compounds. Chemical formula and oxidation state of the carbon atoms are also given.

Compound	Chemical formula	Oxidation state of C
Methane	CH_4	-4
Methanol	CH_3OH	-2
Formic acid (formate)	HCOOH	+2
Formaldehyde	HCHO	0
Formamide	$HCONH_2$	-2
Methylamine	CH_3NH_2	-2
Dimethylamine	$(CH_3)_2NH$	-2
Trimethylamine	$(CH_3)_3N$	-2
Dimethyl ether	$(CH_3)_2O$	-2

For most of the methyl compounds mentioned in table 1.1, carbon has -2 as oxidation state. The lowest possible oxidation state carbon can have is -4 which is obtained in the form of CH_4. The highest possible oxidation state, +4, is obtained in the form CO_2. Complete reduction of CO_2 to CH_4 can release up to 8 electrons, that can be used in energy yielding processes within microbial cells.

While methyl-compounds within organic chemistry often feature simple structures, the biological utilisation of methyl compounds extends to a diverse group of microorganisms. These microbial species may also exhibit facultative methylotrophy, meaning that they are capable of, but not restricted to performing methylotrophic methanogenesis. Some organisms may for instance use both methanol and ethanol as a substrate (Anthony, 1975).

1.3.2 Methanol

Alcohols are compounds that have one or several carboxyl (OH) groups coupled to one or more carbon atoms. The simplest alcohol is the methyl alcohol, methanol. It is a clear and colourless liquid that is easily soluble in water (Ott et al., 2012). It is present in fuels as a petrol additive, used as a carbon source for heterotrophic organisms in the denitrifying step in wastewater treatment, and in many industrial processes.

A dominant cause for loss of methanol in the environment is biodegradation. Methanol can be degraded in both anaerobic and aerobic environments, as many microorganisms produce the enzyme alcohol dehydrogenase. Methanol spills in the environment is not considered particularly toxic, because it is thought to mostly have short term effects, since it readily mixes

with water and rapidly dissipates into the environment and is biodegraded by organisms such as methanogens (Ott et al., 2012).

1.4 Methanogenesis

Methanogenesis is an anaerobic metabolic process that generates methane as the final product of metabolism and is performed exclusively by archaea (Lyu et al., 2018). It constitutes 70-90 % of all methane produced on earth and is significantly contributing to the global methane budget (de Mesquita et al., 2023).

There are three main types of methanogenesis: acetoclastic, hydrogenotrophic and methylotrophic. Acetoclastic methanogenesis uses acetate to generate methane, and hydrogenotrophic methanogenesis uses hydrogen and carbon dioxide. The dominant methanogenic pathway is determined by the relative production rates of the precursors acetate and H_2/CO_2 (Conrad, 2020). Acetoclastic and hydrogenotrophic methanogenesis can be found in many different habitats, from hydrothermal vents in the deep ocean, to the rumen of cattle (Lyu & Liu, 2019).

A general characteristic for all types of methanogenesis is that they have a low net energy yield and are therefore often outcompeted by more energetically favourable metabolisms (Lyu et al., 2018). Methanogenesis is generally common in habitats depleted in energetically advantageous electron acceptors such as O_2, NO_3^-, Fe^{3+} and SO_4^{2-}. For instance, the presence of nitrate tends to favour more energetically favourable metabolisms such as denitrification and dissimilatory nitrate reduction to ammonium (DNRA), thereby hindering methanogenesis (Klüber & Conrad, 1998). Additionally, sulfate reducing bacteria have been shown to outcompete acetoclastic and hydrogenotrophic methanogens whereas methylotrophic methanogens are not as affected by this competition (de Mesquita et al., 2023).

1.4.1 Methylotrophic methanogenesis

Among the three types of methanogenesis, methylotrophic methanogenesis can have the highest net energy yield, depending on the substrate used (Lyu et al., 2018). There are two types of methylotrophic methanogenesis, methyl dismutation and methyl reduction (de Mesquita et al., 2023; Kurth et al., 2020). A simplified pathway for both types of methylotrophic methanogenesis is given in figure 1.2. Methyl reduction is dependent on the availability of H_2, formate, or ethanol as an electron donor. Methyl reduction is therefore viewed as a hydrogen dependent methylotrophic methanogenesis. Methyl dismutation on the other hand oxidizes ¼

of the substrate into CO_2. This process obtains electrons for reduction of the remaining ¾ of the substrate into methane.

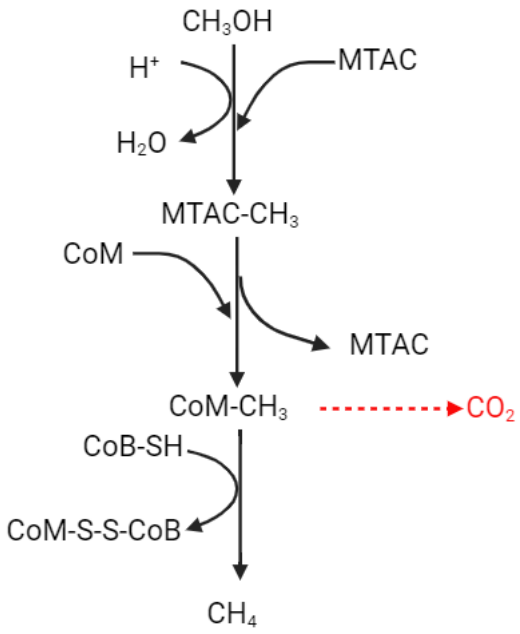

Figure 1.2: Dismutation and reducing pathway of methanogenesis with methanol as substrate. Dismutation where ¼ of the substrate is oxidized to CO_2 to provide electrons is marked in red. Figure was made in BioRender.

Methyl reduction and methyl dismutation utilise all the same enzymes to generate CH_4. However, enzymes involved in the oxidation of ¼ of the substrate into CO_2, are not present in the methyl reduction pathway. The primary step in the formation of methane consists of transferring a methyl group to a substrate-specific corrinoid protein (MTAC), making MTAC-CH_3. The methyl group is then transferred to coenzyme M (CoM) to form methyl coenzyme-M (CoM-CH_3), releasing MTAC in the process. Methyl-CoM reductase will then catalyse the reaction between coenzyme B (CoB) and methyl-CoM to yield methane and generating the heterodisulfide complex CoM-S-S-CoB. This complex has to be reduced before a new methanol molecule can be reduced to methane (de Mesquita et al., 2023; Kurth et al., 2020).

Certain archaea have the genetic potential to not only perform methylotrophic methanogenesis, but also acetoclastic and hydrogenotrophic methanogenesis. Such archaea have a wide variety in substrates they can utilise (Oren, 2014).

1.5 *Methanosarcinaceae*

Methanosarcinaceae is an archaeal family within the order *Methanosarcinales* and the phylum *Euryarchaeota*. *Methanosarcinales* has been identified as a methanogenic order that can utilise a broad range of substrates (Lyu & Liu, 2019; Thauer et al., 2008). Within *Methanosarcinales*, are species that can perform both acetoclastic, hydrogenotrophic and methylotrophic methanogenesis. Members of *Methanosarcinales* have exhibited high resistance to deviations from their optimal growth conditions (De Vrieze et al., 2012). Sudden changes in pH and increases in ammonia levels is not particularly inhibitory for methane production and growth for species within *Methanosarcinales*.

Within the order *Methanosarcinales* is the family *Methanosarcinaceae*, which consists of eight different genera: *Methanococcoides*, *Methanohalobium*, *Methanohalophilus*, *Methanolobus*, *Methanomethylovorans*, *Methanosalsum*, *Methanimicrococcus* and *Methanosarcina*. *Methanosarcina* is one of only two genera of methanogens that can perform acetoclastic methanogenesis (Lyu & Liu, 2019).

Species within *Methanosarcinaceae* grow well on the ocean floor and can survive in a wide range of temperatures and NaCl concentrations (Lyu & Liu, 2019). They are found in a variety of geographic locations such as freshwater, marine and hypersaline sediments, wetlands, thermal environments, oil wells, anaerobic waste treatment systems, and gastrointestinal tracts of animals (Oren, 2014). Certain species in the *Methanosarcinaceae* family are capable of both acetoclastic and methylotrophic methanogenesis from substrates such as methylamines, methanol, or dimethyl sulphide and other species can perform hydrogenotrophic methanogenesis from H_2/CO_2 (Garcia et al., 2000; Oremland & Boone, 1994; Oren, 2014).

There are several possible methylotrophic pathways that still lack to be described either bioinformatically or biochemically (Kurth et al., 2020). Further research regarding methylotrophic methanogens could lead to better understanding of the processes behind the different metabolisms.

1.6 Assessment of taxonomic and metabolic properties

There are a lot of unanswered questions surrounding methylotrophic methanogenesis and pathways used to generate methane. To address these questions, several methods can be employed to assess and characterize the metabolic strategies belonging to methylotrophic methanogens (Dziewit et al., 2015). To better access the microbes, they can be cultivated in microcosms. These microcosms can be amended with different growth substrates, to investigate the effect of enriching for or against a specific metabolism (de Mesquita et al., 2023).

A step in obtaining more knowledge on methylotrophic methanogens can be to sequence their DNA. For instance, information on taxonomic composition, genomic potential and possible metabolic pathways can all be inferred from sequenced DNA (Dziewit et al., 2015). This information can be inferred from a smaller dataset of 16S rRNA samples, or from a larger dataset containing metagenomic data. By selecting suitable databases and software tools, we can gain deeper insights into the microbes performing methylotrophic methanogenesis.

1.6.1 Inferring metabolic information from 16S rRNA analysis

When isolating 16S rRNA sequences to make a community profile, the 16S rRNA sequences are targeted using specific primers. They are amplified using polymerase chain reaction (PCR), followed by sequencing using high-throughput sequencing platforms. Sequencing the 16S rRNA in a sample enables inferring of taxonomic information (Johnson et al., 2019). By using information from literature, it is also possible to correlate the taxonomic information with the metabolic pathways these organisms are known to perform. This approach can provide insights into the metabolic processes that are likely present within the microbial community being studied.

One database that can act as a link between taxonomic information and metabolic function is FAPROTAX (functional annotation of procaryotic taxa) (Louca et al., 2016). FAPROTAX uses published literature from culture studies to infer metabolic strategies to microbial community profiles. The inferring of metabolic information to community profiles using FAPROTAX requires less computing power than metagenomic analyses and might give valuable insight to the community composition and possible metabolic functions. Taxonomic communities in sediment samples can vary significantly, and even though two species are distantly related, they might still perform similar metabolic functions (Martiny et al., 2015).

1.6.2 Determining genetic potential from metagenomic analyses

Unlike 16S rRNA sequencing, which only targets a small part of the genetic content in a sample, metagenomic shotgun sequencing aims to sequence all DNA present in the sample. The sequenced reads can then be assembled into contigs and further into metagenome assembled genomes (MAGs).

The metagenomic approach offers the theoretical capability to capture complete metabolic pathways and gene lists from organisms within the sample. Open reading frames (ORFs) within the MAGs can be annotated into coding sequences and genes by the use of different databases and software (Chen & Pachter, 2005).

Metagenomic analysis requires more computing power compared to 16S rRNA analysis due to its depth and complexity (Laudadio et al., 2018). There are different software available for assembly and annotation of metagenomic data. Certain software are dependent on all genome sequences being fully translated into amino acid sequences before metabolic annotation, while others can work directly with assembled nucleotide sequences.

DRAM (Distilled and Refined Annotation of Metabolism) is a software tool used to annotate genomic data (Shaffer et al., 2020). It takes assembled MAGs as input, and outputs them with metabolic annotations. DRAM employs several software to improve its annotation. Initially, it locates ORFs and predicts the corresponding amino acid sequences. Subsequently, the ORFs are searched for in up to 6 databases: Pfam, KEGG (KO-fam if the user lacks access to KEGG), UniProt, CAZY, MEROPS and VOGDB.

DRAM will provide an annotation table with the top hits from each database. The annotation table includes summary ranks from A to E which specifies the confidences of the annotation. A distillate file is also generated, where genes are categorized to metabolic pathways (Shaffer et al., 2020).

1.7 Aims

The question about how methanol is metabolised in the sea by microbes still remains open. Recent evidence from a master thesis suggests an increase of the relative amounts of methylotrophic methanogens belonging to the order *Methanosarcinales* when marine sediment samples are amended with methanol (Martin, 2023).

We hypothesize that by enriching marine microcosms with methanol, the relative amounts of *Methanosarcinaceae* will increase. By enriching the marine sediments with a methyl compound, in this case methanol, we aim to make conditions favourable for these methanogens.

In this thesis, we aim to genome sequence methylotrophic methanogenic archaea. To accomplish this, marine microcosms will be amended with specific nutrients. In particular, we want to look into archaea belonging to the family *Methanosarcinaceae*. We want to extract DNA from enriched microcosms, and to analyse it using metagenomics. The following sub-goals were addressed:

- Enrich the methanogenic family *Methanosarcinaceae*
- Understand under which conditions *Methanosarcinaceae* is enriched
- Investigate which potential metabolic pathways are used by *Methanosarcinaceae* under the given enrichment conditions

The strategy to achieve these subgoals were as follows:

- Enrich marine microcosms in a specific way that reduces the complexity of the microbial community

- Monitor the microcosms during the enrichment period by measuring different nitrogen-species, pH, and oxidation reduction potential (ORP)
- Extract DNA from the sediments, and perform absolute quantitation using qPCR with specific primers, 16S rRNA amplicon sequencing as well as shotgun metagenome sequencing
- Metagenomic analysis of the marine methanogenic archaea for further characterization and description of genetic potential and taxonomic composition of the sediments

2 Materials & methods

2.1 Overview

Sediment was collected from Håøya – Selskjærsbukta at 30 meters depth and stored at 4 °C for approximately one month. A sample of the sediment was taken as a null sample and frozen in 1:3 (v/v) STAR buffer (Roche Diagnostics, USA). The rest of the sediment was treated as seen in figure 2.1 which is a flow chart for the experimental set up.

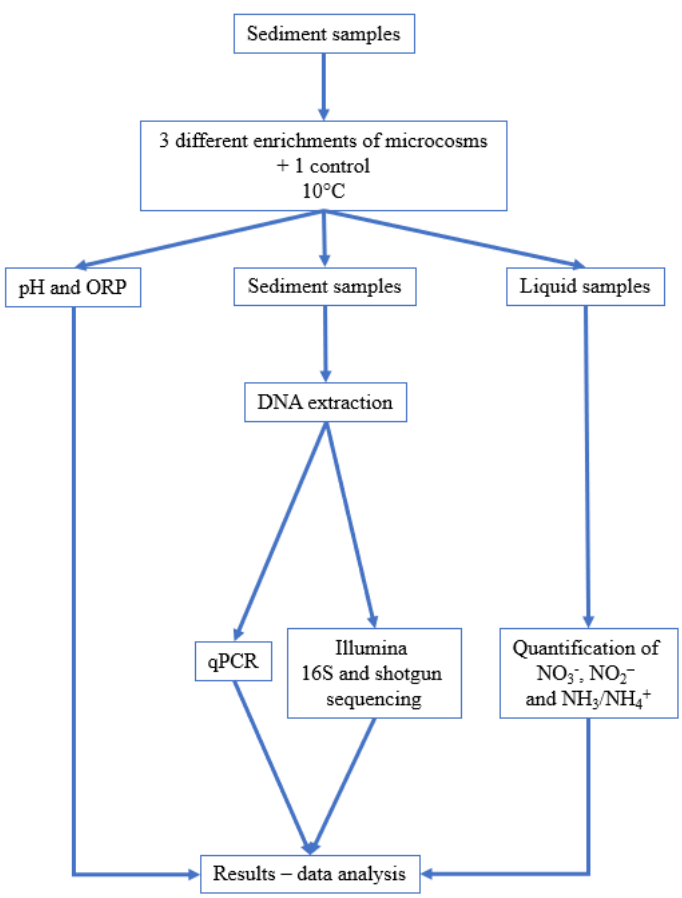

Figure 2.1: Overview of the experiment. Beakers of sediment covered with enriched media were stored in the dark at 10 °C. They were taken out 4 times a week for different measurements, including liquid sampling for quantification of nitrogen-species, pH and ORP measurement and sediment sampling for sequencing. After the data had been collected, data analysis was mainly performed using R version 4.3.3 (R Core Team, 2024). Certain parts of the R analysis were modified from code provided by Julie Martin (PhD).

2.2 Set up of the experiment

2.2.1 Synthetic crenarchaeota saltwater medium

Synthetic crenarchaeota saltwater medium consisting of 26 g/L NaCl, 5 g/L $MgSO_4 \cdot 7H_2O$, 5 g/L $MgCl_2 \cdot 6H_2O$, 1.5 g/L $CaCl_2 \cdot 2H_2O$, 0.1 g/L KBr, mixed with 989.7 ml deionized H_2O was made. The media was autoclaved at 121 °C and cooled to room temperature before adding: 3

ml $NaHCO_3$ (1 M), 5 ml KH_2PO_4 (0.4 g/L), 1 ml FeNaEDTA solution (7.5 mM), 0.2 ml NH_4Cl (1 M) and 0.1 ml α-ketoglutaric acid (100 mM). Lastly, 1 ml trace element solution was added.

A 100 ml trace element solution consisted of 0.8 ml 12.5 M concentrated HCl (0.1 M), 3.0 mg H_3BO_3 (0.48 mM), 10.0 mg $MnCl_2 \cdot 4H_2O$ (0.51 mM), 19.0 mg $CoCl_2 \cdot 6H_2O$ (0.80 mM), 2.4 mg $NiCl_2 \cdot 6H_2O$ (0.1 mM), 0.2 mg $CuCl_2 \cdot 2H_2O$ (0.012 mM), 14.4 mg $ZnSO_4 \cdot 7H_2O$ (0.50 mM), 3.6 mg $Na_2MoO_4 \cdot 2H_2O$ (0.17 mM) and 99.2 ml deionized H_2O. The provided concentrations apply to the 100 ml trace element solution.

The trace element solution was made beforehand. It had been stored in the dark at 4 °C for approximately 20 months. The finished media was stored in the dark at 4 °C.

2.2.2 Microcosm set up

The 3 litres of medium were split into 4 autoclaved blue-cork bottles. The medium was enriched in one of 4 ways:

1. No enrichment (control)
2. Enrichment with methanol (0.1 % v/v)
3. Enrichment with nitrate (0.02 % w/v)
4. Enrichment with methanol and nitrate (same volumes as above).

The experiment was set up as follows: 150 g sediment was added to a 400 ml beaker and covered with 250 ml of the enriched medium. Each enrichment was made in duplicate, and 8 beakers were set up in total. The beakers were covered with aluminium foil and stored in the dark at 10 °C. Nitrogen-species (NO_3^-, NO_2^- and NH_3/NH_4^+) were measured every 3-4 days, and pH and ORP measurements were performed every 1-2 days, aligning with Mondays, Tuesdays, Thursdays, and Fridays.

2.2.3 Sampling and incubation of the microcosms

For the nitrogen measurements, 850 µl was sampled and replaced with the corresponding volume of fresh medium. Nitrite and ammonia were measured the same day as the sampling and nitrate was measured the following day. The liquid samples were stored at 4 °C overnight. After the liquid had been sampled, ORP and pH were measured on top of the sediment using a pH/ORP/Temperature Tester (Hanna Instruments). Sediment samples were taken every 3-4 days, mixed 1:3 (v/v) with STAR buffer (Roche Diagnostics, USA) and stored at -18 °C. All beakers were stored in the dark at 10 °C.

2.3 Nitrogen measurements

To analyse the amounts of nitrate, nitrite, and ammonium in the medium, three different spectrophotometric assays were conducted. A Shimadzu UVmini 1240 UV-VIS spectrophotometer (Shimadzu, Japan) was used for all spectrophotometric measurements.

Stock solutions of 1 M KNO_3, KNO_2 and NH_4Cl were used to make standard curves of each assay. The stock solutions were diluted with milliQ-water to 10 mM (nitrate and ammonium) and 0.5 mM (nitrite). These were used to make standard curves for nitrate (0, 0.05, 1, 2, and 3 mM), nitrite (0, 0.025, 0.05 and 0.1 mM), and ammonium (0, 0.5, 2.5, and 5 mM). The spectrophotometer was calibrated using one 0 mM blank sample. One measurement of a standard was also included every time measurements were performed. Its concentration was 2 mM for NO_3^-, 0.5 mM for NO_2^- and 2.5 mM for NH_4^+. All measurements from medium in the experiment were done in triplicates.

2.3.1 Measuring nitrate

A volume of 4.5 µl reagent A, saturated H_3NSO_3, was mixed with 18 µl sample. Next, 90 µl reagent B, salicylic acid in concentrated H_2SO_4 (5%, w/v), was added and vortexed well before incubating in the dark at room temperature for 10 minutes. Then 900 µl reagent C, 4 M NaOH, was added, and the samples were incubated in the dark for 20 minutes. Absorbance was measured spectrophotometrically at 420 nm. All reagents were stored in the dark, A and C at 4 ℃ and B at room temperature.

2.3.2 Measuring nitrite

Nitrite was measured using the Griess assay. An Eppendorf tube containing 850 µl 1:1 mixture of A: 0.2 g/L N-(1-naphthyl)ethylenediamine dihydrochloride in 1.5 M HCl and B: 10 g/L sulfamic acid in 1.5 M HCl, was added 170 µl sample. The mixture was incubated in the dark at room temperature for 10 minutes, and absorbance was read at 543 nm. All reagents were stored in the dark, A at 4 ℃ and B at room temperature.

2.3.3 Measuring ammonium/ammonia

Ammonium was quantified with the OPA assay. The OPA-reagent consisted of 5.4 g/L ortho-phthalaldehyde ($C_6H_6O_2$) in 10 % ethanol, 360 mM phosphate buffer and 0.5 ‰ β-mercaptoethanol. A mixture of 975 µl OPA-reagent and 65 µl sample was vortexed well and incubated in the dark at room temperature for 20 minutes. Absorbance was measured spectrophotometrically at 420 nm. The OPA-reagent was stored in the dark at room temperature.

2.4 DNA extraction

The sediment samples were thawed on ice. After thawing, approximately 250 µl sediment was mixed 1:3 (v/v) with Bashing Bead Buffer (Zymo Research, USA) in BashingBead Lysis tubes, and stored at 4 °C overnight.

DNA was extracted according to Zymo Research' Quick DNA Fecal/Soil Microbe 96 MagBead kit (Zymo Research, USA) on a KingFisherFlex (Thermo Fisher Scientific, USA). Nuclease-free water was used as negative control, and ZymoBIOMICS Microbial Community Standard (Zymo Research, USA) was used as positive control. For the positive control, 75 µl ZymoBIOMICS Microbial Community Standard was mixed with 175 µl STAR buffer (Roche Diagnostics, USA) before adding to BashingBead Lysis tubes and mixing 1:3 with Bashing Bead Buffer. Samples were lysed in a TissueLyser II (Qiagen, Germany) at 30Hz for 2 x 2.5 min. After lysis, samples were centrifuged at 10,000 g for 1 minute. For extraction, 200 µl supernatant was transferred to wells in a 96-well Deep Well KingFisher sample plate with 600 µl Quick DNA Mag Binding Buffer and 25 µl Mag Binding Beads. The DNA was purified with 900 µl Pre-Wash Buffer, 2 x 900 µl gDNA Wash Buffer and eluted in 60 µl elution buffer.

2.5 Designing primers specifically targeting *Methanolobus*

From the Silva database[1], 28 *Methanolobus* 16S rRNA sequences were downloaded. Geneiuos Prime version 2023.2.1 was used to align the sequences, and to find possible primers. After alignment, sequences shorter than 1350 bases were deleted from the alignment. The specifications set were amplicon length between 150-250 bp, primer length between 18-30 nucleotides, Tm between 65-75 °C, G/C content between 40-60 % and C/G on the 3'-end. Repetitive sequences were avoided as best as possible. In the end one primer pair was selected:

927F: 5'-ATCGCTGAGAGGAGGTGCAT-3'

1171R: 5'-GTGTAGCCCTGGAGATTCGG-3'

When performing a reverse primer BLAST[2] on the primers, only species of *Methanolobus* had a 100% match. Other species within the family *Methanosarcinaceae* had hits with one or more mismatches to either of the forward or reverse primer. Primers were stored at -18 °C.

2.6 Gradient PCR to determine optimal annealing temperature

A gradient PCR master mix consisting of 1x HOT FIREPol Blend Master Mix Ready to Load (Solis BioDyne, Estonia) and 0.2 µM *Methanolobus* primer (forward and reverse) was made.

[1] https://www.arb-silva.de/ (accessed 29.09.2023)
[2] https://www.ncbi.nlm.nih.gov/tools/primer-blast/ (accessed 29.09.2023)

In PCR strips, 23 µl master mix was combined with 2 µl template DNA, either *Methanolobus* gDNA[3] or Zymo Mock Community DNA (Zymo Research, USA). Nuclease-free water was used as a negative control. The PCR cycle was run on a Mastercycler ® gradient 5331 (Eppendorf, USA) using the following program: Initial activation at 95 ℃ for 15 minutes, followed by 30 cycles of denaturation at 95 ℃ for 30 sec, annealing at 43-57 ℃ for 30 sec, and elongation at 72 ℃ for 1 minute. After the 30 cycles, a final elongation was done at 72 ℃ for 10 minutes before cooling to 10 ℃. The products were stored at 4 ℃ after the cycle was done. The PCR products were checked for band formation on a 1.5 % agarose gel at 80V.

2.7 Quantitative PCR (qPCR)

From the result of the gradient PCR, the annealing temperature for all qPCR reactions was set at 57 ℃ to achieve as high specificity as possible of the *Methanolobus* primers. The quantitative PCR master mix consisted of 1x HOT FIREPol EvaGreen PCR supermix (Solis BioDyne, Estonia) and 0.2 µM primer (forward and reverse). In a qPCR plate, 18 µl master mix was combined with 2 µl template DNA. Nuclease-free water was used as a negative control. The PCR cycle was completed using the following program: Initial activation at 95 ℃ for 15 minutes, followed by 40 cycles of denaturation at 95 ℃ for 30 sec, annealing at 57 ℃ for 30 sec, and elongation at 72 ℃ for 45 seconds. High-resolution melting point analysis was performed on all runs. All qPCR runs were performed on a Bio-Rad C1000 Touch™ Thermal Cycler CFX96™ Real-Time System (Bio-Rad, USA).

The sediment DNA was used as template for both short range bacterial PRK341F[4] and PRK806R[5] primers, and *Methanolobus* primers. QPCR analysis was also performed using pure *Methanolobus* gDNA as template as well as *Methanolobus* DNA in a constant diluted background of Zymo mock community DNA to test the affinity of the primers. All plates were stored at 4 ℃ after runs.

2.8 qPCR data interpretation

The raw data from the qPCR runs was uploaded to Bio-Rad CFX Maestro 2.2 version 5.2.008.0222 and fluorescence baseline settings were set to “no baseline subtraction”. Data was further processed using LinRegPCR. The reason for this is that relying on Cq value alone is unwise. Cq is highly reliant on PCR efficiency. When performing qPCR assays, and results are provided only in the form of Cq values, assumptions are made that there has been a 100%

[3] Ordered from https://www.dsmz.de/
[4] 341F: 5’-CCTACGGGRBGCASCAG-3’
[5] 806R: 5’-GGACTACYVGGGTATCTAAT-3’

amplification efficiency. This is most often not the case. PCR artefacts will often reduce the efficiency, and the amplification efficiency is lower in later cycles of the run. If the experiment also relies on several runs and plates, there can be a between-plate-variation that cannot be accounted for when using Cq-values (Ruiz-Villalba et al., 2021).

Therefore, all qPCR results were put through LinReg. LinReg is a linear regression program that will perform a baseline correction on non-baseline corrected qPCR data for each sample individually. It determines the efficiency for each reaction by linear regression, and calculates a corrected Cq value for each sample, called N_0. N_0 provides an estimated starting concentration per sample expressed in relative fluorescence units (RFUs) (Ruijter et al., 2009).

2.9 16S rRNA amplicon sequencing

Amplicon PCR

All PCR runs were performed on a 2720 Thermal Cycler (Applied Biosystems, USA). A reaction mix was made by combining 1x HOT FIREPol Blend Master Mix Ready to Load and 0.2 µM forward and reverse primers. To each well in a 96 well PCR plate, 23 µl the reaction mix, and 2 µl of the extracted template DNA was added. Positive and negative DNA extraction controls were included, as well as Zymo mock community DNA (Zymo Research, USA) and nuclease-free water as positive and negative controls for the PCR run. The primers used were bacterial short range PRK341F and PRK806R. The PCR product was amplified using the following program: Initial activation at 95 °C for 15 minutes, followed by 25 cycles of denaturation at 95 °C for 30 sec, annealing at 55 °C for 30 sec, and elongation at 72 °C for 45 seconds. After 25 cycles, a final elongation was performed at 72 °C for 7 minutes before cooling to 4 °C. Samples were stored at 4 °C overnight.

Clean-up of PCR product using Biomek4000

A subset of the samples were checked on a 1 % agarose gel run at 80 V before the clean-up protocol was started. The clean-up (1:1 v/v magnetic bead clean-up) was performed on a Biomek4000 (Beckman Coulter, USA). Before placing the plate on the robot, 10 µl sample was added 10 µl magnetic beads in a new PCR plate. When on the robot, the sample plate was incubated for 5 minutes, then placed on magnet for two minutes to clear. The supernatant was discarded, and the beads were washed twice with 100 µl 80 % ethanol and left for 30 minutes to air dry. The plate was removed from the magnet and 20 µl water was added, incubated for 2 minutes before placing back on the magnet for 5 minutes. Lastly, 16 µl of the eluate was transferred to a new plate.

Index PCR

A reaction master mix was made for the following PCR reaction, consisting of 1x FIREPol Master Mix Ready to load and nuclease-free water. To each well of the PCR plate 13 µl of the reaction mix was added. Index primers were added using Eppendorf epMotion 5070 robot (Eppendorf, USA), and 2 µl cleaned PCR product was added last. The indexing was performed using the following program: Initial activation at 95 ℃ for 5 minutes, followed by 10 cycles of denaturation at 95 ℃ for 30 sec, annealing at 55 ℃ for 1 minute, and elongation at 72 ℃ for 45 seconds. A final elongation was done at 72 ℃ for 7 minutes before cooling to 4 ℃. All samples were run on a 1.5 % agarose gel at 80 V. Samples were stored at 4 ℃ overnight.

Qubit™ quantitation and library normalisation

A subset of the samples that had the most difference in fluorescence intensity on the gel was measured for DNA concentration using Qubit™ 1X dsDNA HS Assay Kit (Thermo Fischer Scientific, USA). 10 µl standard was mixed with 190 µl working solution, and 2 µl sample was mixed with 198 µl working solution. The tubes where vortexed then incubated in the dark for 2-3 minutes. The standards were used to calibrate the Qubit™ fluorometer before quantitation of the samples.

Indexed amplicons were normalised to approximately 40-50 ng DNA and pooled using a Biomek3000 (Beckman Coulter, USA).

Magnetic bead clean-up of pooled library

To remove unwanted product in the sample, the pooled library was cleaned using 0.1 % Sera Mag Speed Bead solution. Room tempered magnetic beads at a concentration of 0.8X were added to 165 µl of the pooled sample and mixed. The tube was incubated in room temperature for 5 minutes before being placed on a magnetic stand to clear. With the tube on the magnetic stand, the supernatant was discarded, and the beads washed twice with 200 µl freshly prepared 80 % ethanol without resuspending the beads. After the second wash, the tube was left on the magnet for 15 minutes to air dry. The tube was removed from the magnet, and the beads were resuspended in 40 µl nuclease-free water. The tube was incubated at room temperature for 2 minutes before being placed back on the magnetic stand to clear up. Once clear, 35 µl supernatant was transferred to a new tube. Sample concentration was measured by Qubit™ and product size checked on a 2 % agarose gel run at 80 V.

2.10 16S rRNA amplicon data analysis

Amplicon library samples were sequenced by the Norwegian sequencing centre (Oslo university hospital). The resulting files from the sequencing were analysed using the "Amplicon Illumina data processing at MiDiv" pipeline (Lars Snipen, 2023[6]).

The resulting read files were first demultiplexed using R version 4.3.1 (R Core Team, 2024) and RStudio (2023.12.0+369) and quality checked and trimmed using VSEARCH (vsearch:2.22.1--hf1761c0_0, (Rognes et al., 2016)). The reads were trimmed 20 bases of the 3'-end and 60 bases from the 5'-end. This process aimed to eliminate low-quality segments while retaining sufficient overlap for successful assembly. Other specifications set in VSEARCH was that all reads shorter than 200 bp were discarded, and maximum error probability was set to 0.1 (equals quality score of 20). Also, the minimum number of copies a centroid sequence could have, was set to 2, OTU-identity at 0.97 and UNOISE α parameter was set as 2.0.

The OTUs (operational taxonomic units) from the VSEARCH pipeline was then subjected to taxonomic classification (using R version 4.3.2) using SINTAX (implemented in VSEARCH), where the cutoff was set to 0, which allowed for manual filtering at a later stage. The database used for taxonomic classifications (rdp_16s_v18.fa) classifies the OTUs to genus level. The output from SINTAX was analysed using R version 4.3.3 (R Core Team, 2024) and RStudio and all hits with a genus score lower than 0.8 was set as "unclassified". Before further analysis, eukaryotic phyla, and photosynthetic species were removed from the data, and read counts were normalised using total sum scaling (TSS). Samples with a total read count less than 15 000 reads were removed from the dataset, and only sediment samples were kept.

Functional annotation of the amplicon data (FAPROTAX analysis, (Louca et al., 2016)) was performed on a phyloseq object made from the data (McMurdie & Holmes, 2013). To achieve this, the ribosomal RNA Operon copy number database (rrnDB, (Stoddard et al., 2015)) was downloaded and used to convert the 16S rRNA abundances to relative genome abundances. Of all the OTUs, 94 % did not have a hit in the rrnDB database. The average gene copy number in rrnDB was used to calculate the genome abundance of the OTUs that did not have any hits in the database. The FAPROTAX database was used to functionally annotate the OTUs in the data

[6] Amplicon Illumina data processing at MiDiv (nmbu.no)

(Louca et al., 2016). All species names were removed from the database as no species information is provided from the phyloseq object.

Unclassified OTUs from the genus annotation (with a score less than 0.8) were saved to a separate table. These OTUs were attempted classified at family level, and again at order level if no classification on family level was achieved.

At genus level, 60 % of classified genera were successfully matched, equating to 6 % of the initial number of OTUs. At family level, 26 % of classified families were successfully matched, equating to 3 % of the initial OTUs. At order level, 10 % were matched, equating to 2 % of the total number of OTUs. When all functional annotation was finished, abundances were normalised by TSS normalisation.

Relative abundances were plotted using functions from the ggplot2 package (Wickham, 2016).

2.11 Shotgun sequencing

A subset of the samples were selected for sequencing. These were samples from the start, midpoint, and end of the enrichments containing methanol (both methanol and nitrate + methanol) – since there were two parallels, 12 samples were put through the following protocol. The samples selected were submitted to the Nextera DNA Flex Library Prep Protocol.

DNA quantification and tagment genomic DNA

Extracted DNA from the samples that were going to be shotgun sequenced was quantified using Qubit™. From the Qubit™ concentrations, volumes corresponding to 2-6 ng DNA were pipetted out. Volumes were all adjusted to 30 µl with nuclease-free water. A tagmentation master mix was made by mixing equal volumes of Bead-Linked Transposomes (BLT) and Tagmentation Buffer 1 (TB1), enough for all samples including reagent overage to ensure accurate pipetting. To each sample, 20 µl of the tagmentation master mix was added and pipetted to mix. The plate was sealed and run on a 2720 Thermal Cycler (Applied Biosystems, USA) using the TAG program: Preheated lid to 100 °C, 55 °C for 15 minutes and hold at 10 °C.

Post tagmentation clean-up

After tagmentation all samples were added 10 µl Tagment Stop buffer (TSB). The plate was run on the PTC program on the thermal cycler: Preheated lid to 100 °C and held at 37 °C for 15 minutes then held at 10 °C. After the PCT program, the plate was placed on a magnetic stand until the liquid was clear, and the supernatant was discarded. Samples were washed twice, by removing the plate from the magnetic stand, and resuspending the beads in 100 µl Tagmentation Wash Buffer (TWB) before being placed back on magnet, and discarding the supernatant when

the liquid was clear. After clean-up, the beads were resuspended in 100 µl TWB and the sealed plate was placed on the magnetic stand until ready to continue with the next step.

Amplifying tagmented DNA

A 1:1 mix of Enhanced PCR Mix and nuclease-free water was made, enough for all samples including reagent overage. The TWB was removed from the beads, and 40 µl PCR mix was immediately added. The plate was sealed and centrifuged before adding index primers. Primers used were IDT for Illumina Nextera DNA UD Indexes Set C (96 indexes). The samples were mixed by pipetting and centrifuged before running the following BLT PCR program: Preheated lid to 100 ℃, 68 ℃ for 3 minutes, 98 ℃ for 3 minutes and 12 cycles of 98 ℃ for 45 seconds, 62 ℃ for 30 seconds and 68 ℃ for 2 minutes, before 68 ℃ for 1 minute and lastly hold at 10 ℃.

The number of cycles were dependent on the total DNA input (ng) in the samples. The DNA content was between 1-9 ng and therefore submitted to the maximum number of cycles, 12.

Library clean-up

The samples were run on a 2 % agarose gel at 80 V to check fragment dispersion. The plate was then centrifuged before being placed on a magnetic stand to clear. 40 µl from each well was transferred to the corresponding well on a new plate. The samples were cleaned using 1.8 X Sample Purification Beads (small PCR fragment clean up). Each well was added 72 µl Sample Purification Buffer and mixed by pipetting. The plate was incubated at room temperature for 5 minutes, before it was placed on magnet to clear. The supernatant was discarded, and the samples were washed twice with freshly prepared 80 % ethanol. The plate was kept on magnet while 200 µl ethanol was added (without resuspending the beads) and incubated for 30 seconds before removal. The plate was left on magnet to air dry for 5 minutes. Lastly, the plate was removed from the magnetic stand, and the beads were resuspended in 32 µl Resuspension Buffer. After 2 minutes of incubation at room temperature, the plate was placed on the magnetic stand and when the liquid was clear, 30 µl was transferred to a new PCR-plate. The plate was stored at -18 ℃.

Pooling libraries

The DNA content was quantified using Qubit™, and samples were pooled based on their concentrations. Samples were pooled so that all samples contributed with approximately 200 ng DNA. The pooled library was quantified using Qubit™ and run on a 2 % agarose gel at 80 V. The pooled library was stored at -18 ℃.

2.12 Shotgun data analysis

The shotgun samples were sequenced by Novogene. The resulting files from the sequencing were analysed using "Illumina metagenome processing – MAGmachine" pipeline (Lars Snipen[7]). First a read quality inspection was performed using fastqc (fastqc:0.11.9--hdfd78af_1), to generate HTML-files containing quality information. The reads were then trimmed for adapter sequences, filtered for read quality, and ends of poor quality were trimmed using bbduk (bbmap:39.01--h5c4e2a8_0). No bases were trimmed off the 5'-end and read bases extending beyond base 150 were trimmed.

Then the read-pairs that happened to overlap were merged using bbmerge (same version as bbduk) (Bushnell et al., 2017). This reduces the memory load for metaspades in the next step. Metaspades (spades:3.15.5--h95f258a_1, (Nurk et al., 2017)) was used for assembly of all reads from each sample into contigs. Following this, both metabat2 (metabat2:2.15--h986a166_1) and maxbin2 (maxbin2:2.2.7--he1b5a44_2) were utilised to merge all contigs into bins (Kang et al., 2019; Wu et al., 2016). The last procedure performed was to assign bins into MAGs. All bins were quality assessed using checkm2 (checkm2:1.0.1--pyh7cba7a3_0, (Chklovski et al., 2023)), re-replicated using dRep (drep:3.4.0--pyhdfd78af_0, (Olm et al., 2017)) and assigned taxonomy using gtdbtk (gtdbtk:2.3.2--pyhdfd78af_0, (Chaumeil et al., 2020)). The minimum completeness was set at 75% and max contamination at 25% for the bins to qualify for MAG assembly.

DRAM was used to metabolically annotate the MAGs. The minimum contig length parameter was reduced from default 2000 to 500 (Shaffer et al., 2020).

2.13 Statistical analysis

Due to the low number of samples and dependencies in the data, Wilcoxon non-parametric signed rank tests were performed. Pairwise tests were conducted to see whether the enrichment conditions had a significant effect on the relative abundances of methanogenic archaea, particularly archaea within the family *Methanosarcinaceae.* Tests were also performed across all OTUs to assess differential abundance under each enrichment condition. The corresponding p-values were adjusted using Benjamini & Hochberg correction, also called fdr or false discovery rate correction (Benjamini & Hochberg, 1995).

[7] https://arken.nmbu.no/~larssn/MiDiv/README_metagenomes.html

3 Results

3.1 ORP and pH measurements in the enrichment

Oxidation reduction potential (ORP) and pH was measured simultaneously through the incubation period, shown in figure 3.1A and 3.1B. The initial pH measurements for all enrichments ranged between 8.01 and 8.11, with a slight drop in pH in the beginning of the incubation period. The measurements are plotted to start at day -4, to align with the data from the amplicon and shotgun analyses which start at day 0.

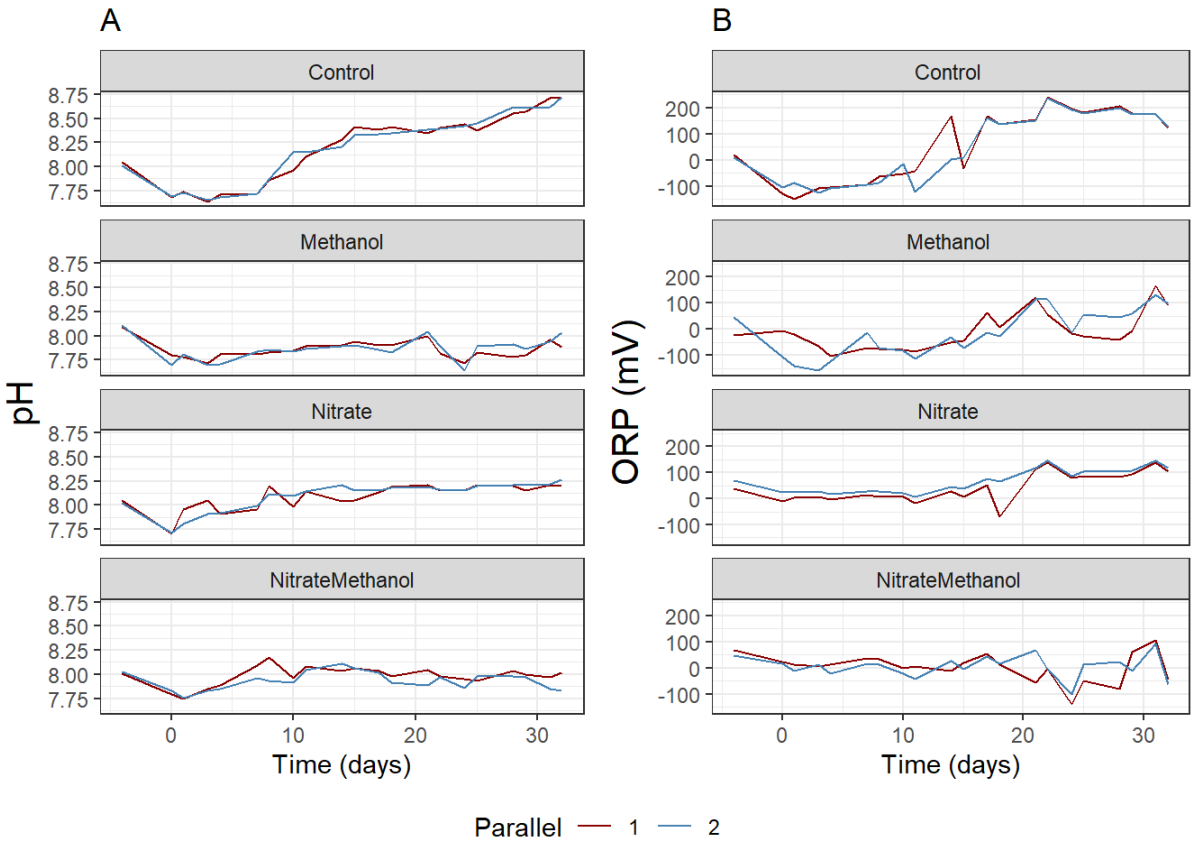

Figure 3.1: Measurements of pH and oxidation reduction potential (ORP) throughout the incubation period. Measurements were performed four times per week. Parallels are plotted together, red lines represent parallel 1, and blue lines parallel 2.

The pH of the control enrichment initially decreased to about 7.70 before steadily rising for the remainder of the incubation period. Similarly, the initial ORP values for the control were approximately +20 mV, subsequently decreasing to around -140 mV before ultimately returning to +170 mV, concurrent with the pH changes. The nitrate enrichment had stable pH and ORP through the incubation. The enrichments containing methanol (both methanol and nitrate + methanol) had lower pH measured throughout the incubation compared to the control and nitrate enrichments. Generally, the pH and ORP within a treatment followed similar trends, but

for the methanol enrichment, the ORP started increasing midway through the incubation, which was not observed for the pH.

3.2 Nitrogen measurements

The calculated concentrations of the spectrophotometric measurements of nitrate (A), nitrite (B) and ammonia (C) are shown in figure 3.2. The synthetic seawater media had 0.2 mM ammonia added. This is reflected in figure 3.2C. The beakers enriched with nitrate were added 0.2 mM. No nitrite was added in any of the beakers.

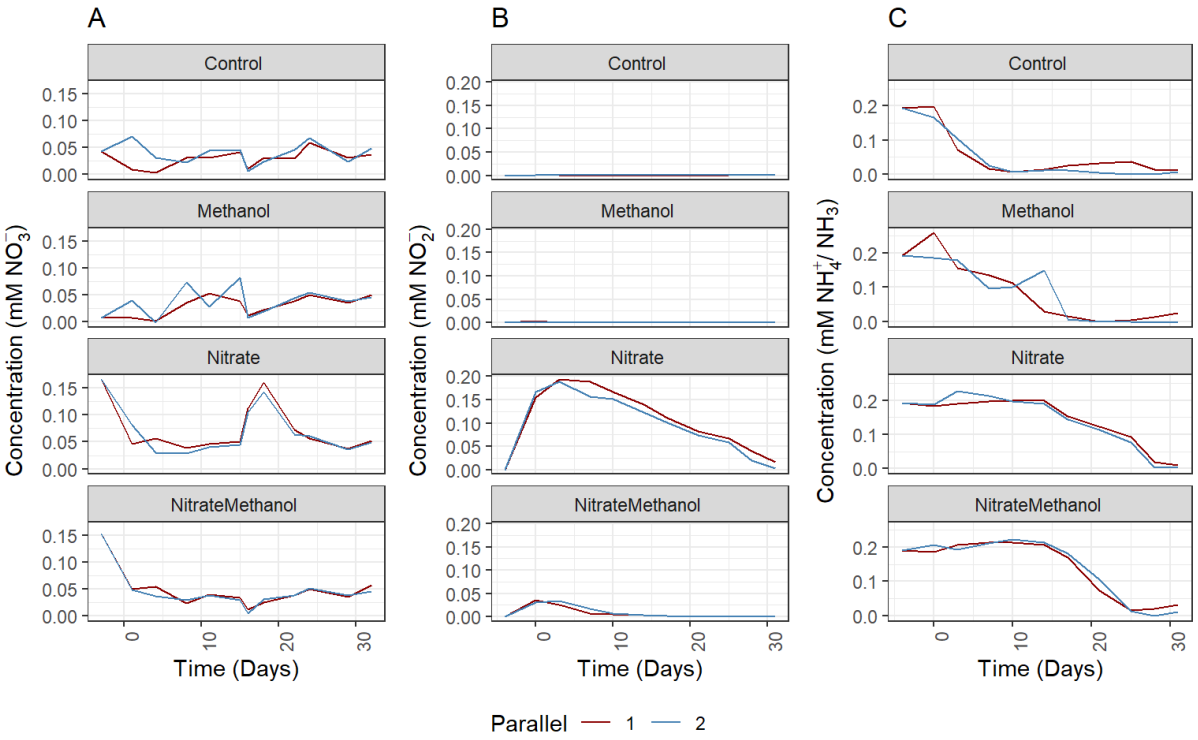

Figure 3.2: Calculated concentrations of nitrate, nitrite, and ammonia/ammonium throughout the incubation period. Measurements were performed every 3 to 4 days. Concentrations were calculated from spectrophotometric absorbance and standard curves for each assay. Parallels are plotted together, red lines represent parallel 1, and blue lines parallel 2. Standard curves are given in the appendix.

In general, the nitrate concentrations sank rapidly for the nitrate and the nitrate + methanol enrichments and stabilised at approximately 0.05 mM from day 0 onwards. The methanol enrichment had a slight increase of nitrate, from 0 mM to 0.05 mM. The control enrichment measured approximately 0.05 mM the entire incubation. There were some deviations between the parallels for the control and the methanol enrichments. Standard deviations for the triplicate measurements for the nitrate enrichment were the largest of the three assays with 14 measurements having a standard deviation higher than ±0.040 mM.

In the control and the methanol enrichments, no nitrite was detected throughout the entire incubation period. In the nitrate + methanol enrichment, there was a slight increase in nitrite

concentration from the first to the second sample day, reaching a maximum concentration of 0.030 mM before decreasing over the next 14 days. The beakers that were only enriched with nitrate, had a higher peak of nitrite accumulation. The highest measured average nitrite concentration was 0.19 mM in parallel 2 at day 3. From this point onwards, the concentration decreased steadily until the end of incubation. The triplicate nitrite measurements had lower standard deviations compared to the measurements of nitrate. The highest calculated standard deviation was ±0.0033 mM. The high standard deviation originated from the measurements where the nitrite concentration was highest (in the nitrate enrichment). All other standard deviations were equal to or less than ±0.0006 mM. The variation between the parallels was also smaller in the nitrite assay compared to the nitrate assay.

The ammonia concentrations decreased to 0 mM at different rates in each enrichment. For the control enrichment, the ammonia concentration became undetectable at day 10. For the methanol enrichment, the same happened at day 21. In the nitrate-containing enrichments, ammonia concentrations exhibited a slower reduction rate, reaching 0 mM at day 28 and 31. Specifically, the nitrate enrichment degraded ammonia to undetectable limits by day 31, while the nitrate + methanol enrichment obtained 0 mM concentrations of ammonia by day 28. Compared to the control, the degradation of ammonia took approximately twice as long in the methanol enrichment and three times as long in the nitrate enrichments (both nitrate and nitrate + methanol). The triplicate measurements in all enrichments had lower standard deviations than the nitrate measurements, with only one calculated deviation being higher than ±0.017 mM. The variation between the parallels was also smaller compared to the nitrate assay, except for two measurements in the methanol enrichment, at day 0 and day 7, seen in figure 3.2C.

3.3 Determining taxonomy from 16S rRNA sequences

Before the enrichment experiment was set up, a null sample was taken from the sediment. The relative abundances of the families in this sample is plotted in figure A2. The relative abundances were highest for OTUs belonging to the families *Desulfobacteraceae*, *Desulfobulbaceae* and *Ectothiorhodospiraceae*. These three families covered approximately 0.25 of the total relative abundance.

3.3.1 PCoA analysis

From this point onwards, the null sample is not included in any analyses. The null sample was taken at day -4, concurrent with the timeline in figure 3.1 and 3.2. The sampling of the sediment after experiment enrichment and set up started at day 0.

A Principal Coordinate Analysis (PCoA) based on Bray-Curtis distances was performed to assess differences in composition of the enrichments. Figure 3.3 illustrates the results of this analysis. The two primary PCoA components are plotted against time, with PCo1 accounting for 32.8 % and PCo2 15.4 % of the variation in the data. In plot A, PCo1 is plotted against time, in plot B, PCo2 against time.

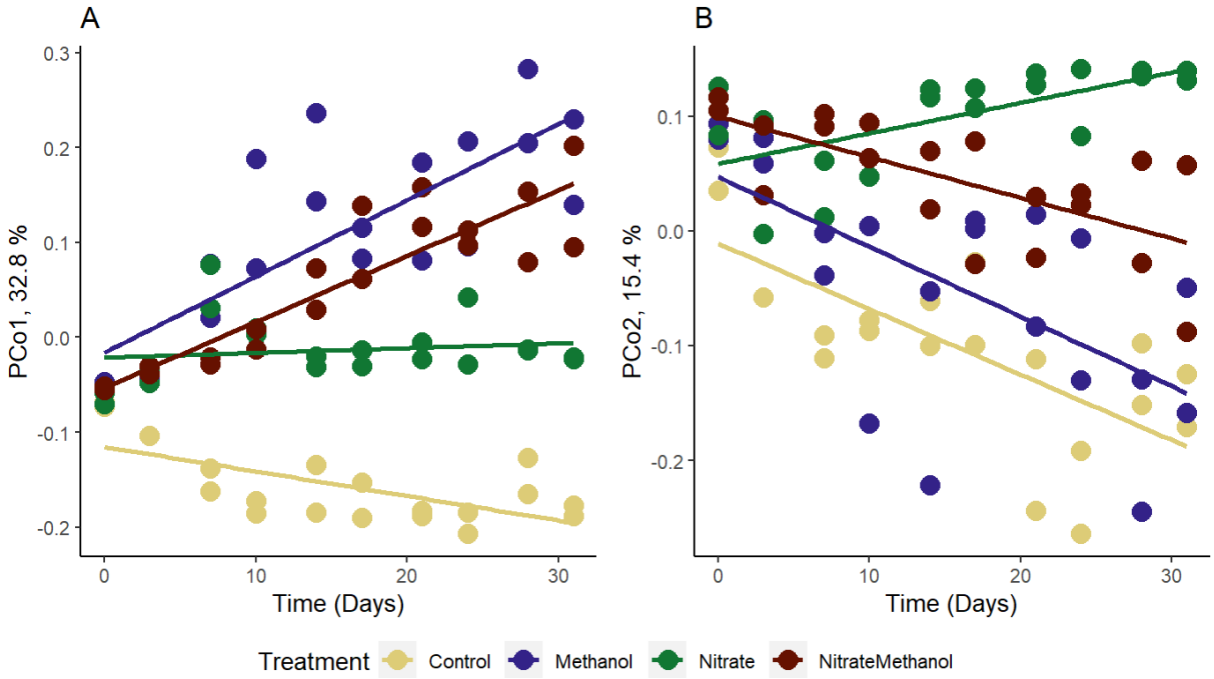

Figure 3.3: A principal coordinate analysis (PCoA) plot from Bray-Curtis distances. Each colour represent a treatment. PCo1 cover 32.8% and PCo2 15.4% of the variation in the data. Linear trend lines are included.

From figure A, PCo1 primarily captures variation between samples enriched in methanol and the remainder of the treatments. The methanol enriched samples have a positive trend on the PCo1 axis, with the nitrate enrichment having a slightly positive trend, and the control enrichment a negative trend. In plot B, PCo2 is more explanatory for the variation between the nitrate enrichment and all other enrichments. Only the nitrate enrichment has a positive trend in plot B, and all other enrichments have a negative trend.

3.3.2 Taxonomic analysis

Figure 3.4 visualise the top 10 most abundant Operational Taxonomic Units (OTUs) in each treatment. The OTUs have been taxonomically classified to their respective families. One sample from the control was removed, due to it having a too low total read count. The total relative abundance covered by the top 10 OTUs varied across different samples within each treatment.

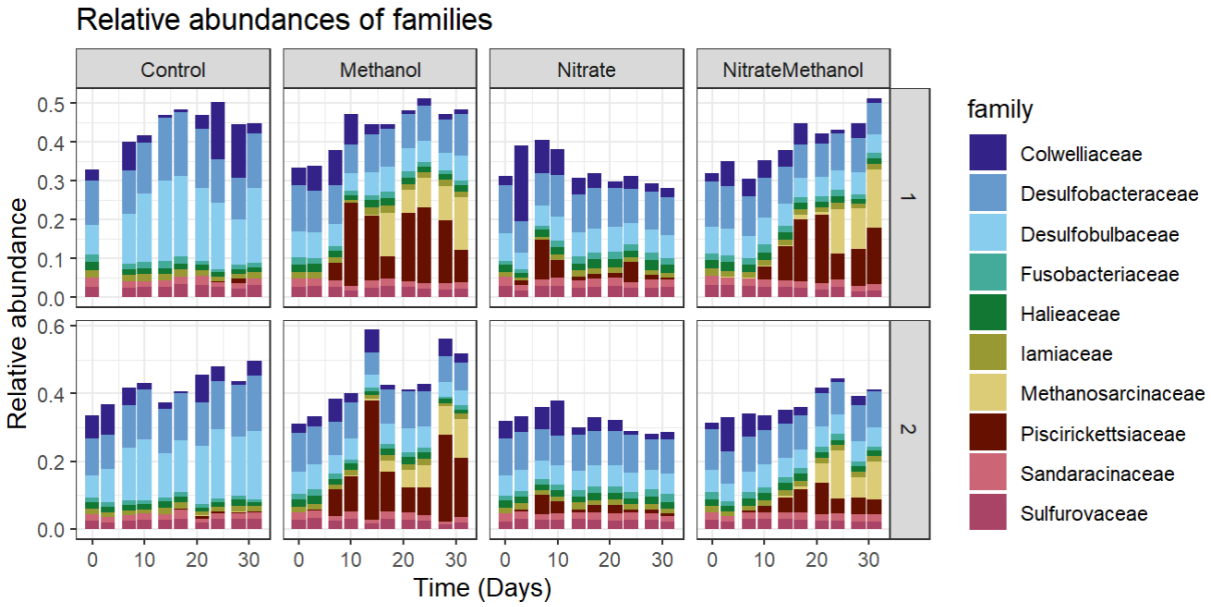

Figure 3.4: Bar charts of the top 10 most abundant families in the samples, split by treatment type and parallel.

The relative abundances of the top 10 OTUs in the control enrichment remained stable through incubation. The families *Colweillaceae*, *Desulfobacteraceae* and *Desulfobulbaceae* were present in all samples and constituted the majority of the relative abundances. The diversity in the control enrichment decreased over time as the top 10 most abundant OTUs covered more of the total relative abundance.

The most relative abundant families in the nitrate enrichment were similar to what was detected in the control enrichment. The three most abundant families were *Colweillaceae*, *Desulfobacteraceae* and *Desulfobulbaceae*. The trend for the abundances in the nitrate enrichment was the opposite of what was seen in the control. The diversity increased over time, as the top 10 most abundant OTUs accounted for a smaller proportion of the total relative abundance.

In the initial samples from the methanol enrichment, the composition of the top 10 most abundant OTUs closely resembled those in the control. However, from day 7 there was an increase of the family *Piscirickettsiaceae*, and at day 16, the family *Methanosarcinaceae* was

also detected. *Methanosarcinaceae* is a methanogenic archaeal family able to perform methylotrophic methanogenesis (Allen et al., 2009). A Wilcoxon signed rank test on the relative abundances of *Methanosarcinaceae* yielded a p-value of $8.34 \cdot 10^{-7}$.

The top 10 most relative abundant OTUs in the nitrate + methanol enrichment exhibited similar patterns as observed in the methanol enrichment. The family *Piscirickettsiaceae*, increased in relative abundance from day 10, and *Methanosarcinaceae* from day 21 (p-value of $5.64 \cdot 10^{-7}$). Similar statistical testing for the nitrate enrichments yielded a not statistically significant p-value. When testing for significant difference in presence of *Methanosarcinaceae* for the control, paired testing was only possible for parallel 2 since parallel one had been stripped of one sample. The test for parallel 2 of the control enrichment, yielded a p-value 0.0059.

When plotting the relative abundance of only *Methanosarcinaceae* over time, the increase in abundance of this archaeal family becomes more visible. This is illustrated in figure 3.5. *Methanosarcinaceae* could be found in all enrichments, but in negligible amounts in the control and nitrate enrichments. The highest relative abundance found for *Methanosarcinaceae* in the control sample was $3.36 \cdot 10^{-3}$ and $7.85 \cdot 10^{-5}$ for the nitrate enrichment. *Methanosarcinaceae* was more abundant in enrichments containing methanol, particularly in later stages of the incubation. Both enrichments containing methanol, experienced a steep increase of relative abundance of *Methanosarcinaceae*, to a maximum of 0.14 and 0.15 in the last sampling in parallel 1 for both enrichments. An earlier increase in relative abundance of *Methanosarcinaceae* was observed in the methanol enrichment compared to nitrate + methanol.

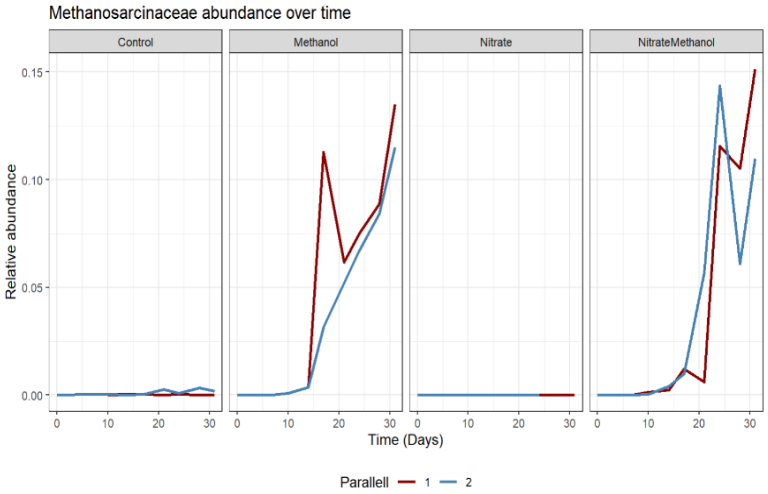

Figure 3.5: Line plot of family Methanosarcinaceae over time in each enrichment. Parallels are plotted together, red lines represent parallel 1, and blue lines parallel 2.

3.3.3 Inferring methylotrophic functional groups

From the FAPROTAX analysis, methylotrophic metabolisms were isolated. The metabolisms isolated in figure 3.6 are methanogenesis and methanol oxidation. Methanogenesis was divided in 4 different groups: 1) methanogenesis, 2) methanogenesis by CO_2 reduction with H_2, 3) methanogenesis by disproportionation of methyl groups (methyl dismutation), and 4) methanogenesis by reduction of methyl compounds with H_2 (methyl reduction).

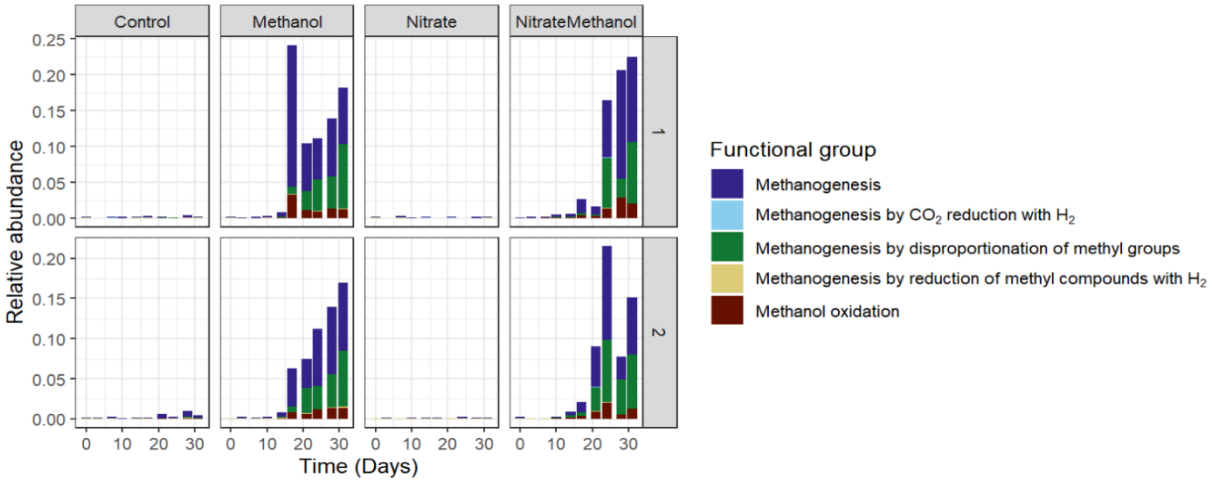

Figure 3.6: Functional groups related to methanogenesis, and methanol oxidation in each enrichment and parallel.

When isolating methanogenesis and methanol oxidation, the nitrate and control enrichment had very low total relative abundances. The highest total relative abundance recorded was 0.0097 for day 29, parallel 2 in the control enrichment. The methanol and nitrate + methanol enrichments had an increase in the relative abundance of organisms performing different types of methanogenesis and methanol oxidation. “Methanogenesis” and “methanogenesis by disproportionation of methyl groups” increased from day 17 in the methanol enrichment. The nitrate + methanol enrichment had a similar increase in relative abundances of these functional groups mainly from day 21. The increase of methanogenic metabolisms in figure 3.6 is happening at the same days the increase of *Methanosarcinaceae* is detected in figure 3.5 and 3.4.

3.3.4 Differential abundance

Wilcoxon signed rank tests were performed across all OTUs to determine significant differences in relative abundance between each enrichment and the control. Between the methanol and control enrichment, 39 OTUs were identified as significantly different, shown in figure 3.7A. Positive differential abundance indicated that the relative abundance of the OTU was higher in the enriched samples compared to the control. There were 6 OTUs that had positive differential abundance. They belonged to three different families: *Oceanospirillaceae*, *Piscirickettsiaceae* and *Methanosarcinaceae* and their mean relative abundance is visualised in figure 3.7B. *Oceanospirillaceae* had the smallest change in relative abundance, with the mean relative abundance reaching a maximum of 0.022 at day 7 before decreasing. The relative abundance of *Piscirickettsiaceae* and *Methanosarcinaceae* increased through the incubation, and *Piscirickettsiaceae* reached a maximum relative abundance of 0.13 by day 14. *Methanosarcinaceae* increased towards the end of the incubation and reached a maximum relative abundance of 0.084 at day 31.

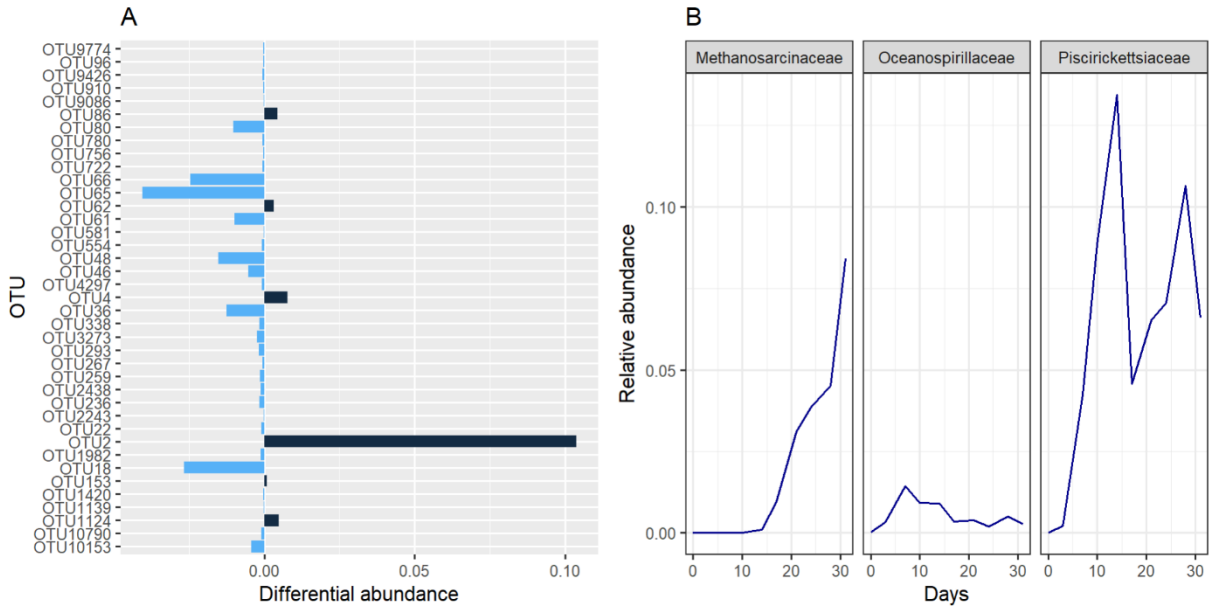

Figure 3.7: Differential abundance analysis across all OTUs belonging to the methanol and the control enrichment. Figure A show all the OTUs with a significantly differential abundance. Figure B illustrate the relative abundance over time of the families that had a positive differential abundance.

The same differential abundance analysis for the nitrate + methanol enrichment, output a higher number of differentially expressed OTUs. The amount of OTUs that had a positive differential abundance in the nitrate + methanol enrichment were 62 compared to 6 in the methanol enrichment. *Piscirickettsiaceae* and *Methanosarcinaceae* were among the 8 most differentially abundant families. They had the biggest changes in relative abundance of all the positively differentially expressed OTUs in the nitrate + methanol enrichment. *Methanosarcinaceae*

reached a higher average relative abundance than *Piscirickettsiaceae* in the nitrate + methanol enrichment.

In the same differential abundance analysis for the nitrate enrichment, the number of OTUs that had positive differential abundance were 160. *Piscirickettsiaceae* was one of the most differentially expressed families, but *Methanosarcinaceae* was not detected among the differentially abundant OTUs.

3.4 Shotgun data analysis

Of the 81 sediment samples taken throughout the incubation period, 12 were shotgun sequenced. Since the focus was on the family *Methanosarcinaceae*, samples were chosen so that the likelihood of getting MAGs (metagenome assembled genome) from this family was higher. From the qPCR results using *Methanolobus* primers an increase of N_0 was detected from the midpoint of the analysis for the methanol and the nitrate + methanol enrichment. Samples from the beginning, midpoint, and end point from both parallels of these two enrichments – corresponding to day 0, 14 and 31 were selected for sequencing.

From the 12 samples, 15 MAGs were output. The 15 MAGs originated from 6 unique samples. Twelve of the MAGs were bacterial, and three were archaeal. Table 3.1 gives an overview of all MAGs, including the highest taxonomic classification, completeness and contamination determined from the MAG assembly, as well as a MAG-name and the genome size.

Table 3.1: Overview of all MAGs output from the shotgun pipeline. The highest taxonomic classification for each MAG is given together with the taxonomic level. Genus (g), family (f), order (o) and class (c). The three first MAGs are from the domain *Archaea*, the rest from the domain *Bacteria*.

MAG-name*	Highest tax. classification	Completeness (%)	Contamination (%)	Size (Mbp)
M.31.2A **	g: *Methanococcoides*	97.00	18.46	4.45
NM.31.1A **	g: *Methanococcoides*	92.13	11.95	3.45
NM.31.1B **	g: *Methanolobus*	96.39	0.00	2.14
M.14.2A	o: *Polyangiales*	76.33	20.85	7.00
M.14.2B	f: *Methylophagaceae*	100.00	0.00	2.42
M.31.1A	f: *Sedimenticolaceae*	86.46	17.88	4.14
M.31.1B	f: *Desulfocapsaceae*	84.72	19.86	4.38
M.31.1C	o: *Bacteroidales*	76.28	10.92	6.39

M.31.2B	f: *Flavobacteriaceae*	100.00	24.90	7.48
NM.0.1A	o: *Arenicellales*	76.36	15.26	5.72
NM.0.1B	c: *Thermoanaerobaculia*	81.42	16.48	7.75
NM.0.1C	c: *Acidimicrobiia*	77.65	19.15	6.66
NM.31.1C	f: *Methylophagaceae*	85.15	12.07	6.69
NM.31.1D	o: *Polyangiales*	79.11	19.23	5.66
NM.31.2	c: *Thermoanaerobaculia*	85.09	16.67	8.28

***** The MAGs were named using 4 factors. 1) the enrichment they originated from, M (methanol) or NM (nitrate + methanol), 2) the day it originated from, 3) the parallel it originated from and 4) a letter (A, B, C or D) to separate MAGs from the same treatment, day and parallel.

****** Archaeal MAGs from the sequencing. These are the MAGs in focus in the later sections.

All archaeal MAGs belonged to the family *Methanosarcinaceae*. They were the only MAGs that were classified to genus level, and the genus was either *Methanococcoides* (2) or *Methanolobus* (1). The completeness was above 92 % and contamination was less than 20 % for all the archaeal MAGs. *Methanococcoides* M.31.2A and *Methanococcoides* NM.31.1A were assembled from bins by maxbin2 and *Methanolobus* NM.31.1B from metabat2. *Methanococcoides* NM.31.1A and *Methanolobus* NM.31.1B were from parallel 1, day 31 from the nitrate + methanol enrichment. *Methanococcoides* M.31.2A was from the sample corresponding to parallel 2, day 31 of the methanol enrichment.

The archaeal MAGs were analysed using DRAM. The three MAGs gave varying outputs: DRAM annotated 7119 genes for *Methanococcoides* M.31.2A, 5725 genes for *Methanococcoides* NM.31.1A and 2080 genes for *Methanolobus* NM.31.1B.

3.4.1 Methanogenesis in the MAGs

Methanolobus NM.31.1B had 153 energy generating genes and the most methanogenesis genes identified of all the MAGs at 105. *Methanococcoides* M.31.2A had 176 energy generating genes and 80 methanogenesis genes, while for *Methanococcoides* NM.31.1A 202 energy generating genes and 82 methanogenesis genes were identified.

Methanococcoides NM.31.1A had a genome size of 3.45 Mpb, and *Methanococcoides* M.31.2A had 4.45 Mbp. The genome size of *Methanolobus* NM.31.1B was 2.14 Mb which was less than half the size of the largest archaeal MAG.

Of the 105 identified methanogenesis genes in *Methanolobus* NM.31.1B, 20 were annotated to methanogenesis using methanol as substrate. *Methanococcoides* M.31.2A contained 80

methanogenesis genes in total, of which 10 were related to methanogenesis using methanol as substrate. For *Methanococcoides* NM.31.1A the corresponding numbers were 82 and 11.

A total of 13 unique genes were found when investigating genes related to methanogenesis using methanol as substrate. *Methanococcoides* M.31.2A and *Methanococcoides* NM.31.1A had 9 unique genes, and *Methanolobus* NM.31.1B had 13 unique genes. The genes are shown in table 3.2.

Table 3.2: Table of all genes from the three archaeal MAGs that were related to methylotrophic methanogenesis from methanol. The coloured rows in the table represent genes that belong to the same enzyme or that work together to perform a specific function in the methanogenesis pathway. The number of gene copies found in the MAGs are given under each MAG-name.

KO_id	KEGG hits	NM.31.1A	NM.31.1B	M.31.2A	
K00125	formate dehydrogenase (coenzyme F420) β subunit	0	1	0	fpo
K00399	methyl-coenzyme M reductase α subunit	1	1	1	mcrA
K00401	methyl-coenzyme M reductase β subunit	1	1	1	mcrB
K00402	methyl-coenzyme M reductase γ subunit	1	1	1	mcrG
K03388	heterodisulfide reductase subunit A2	0	2	0	hdrA
K03389	heterodisulfide reductase subunit B2	0	2	0	hdrB
K03390	heterodisulfide reductase subunit C2	1	2	1	hdrC
K08264	heterodisulfide reductase subunit D	2	3	1	hdrD
K08265	heterodisulfide reductase subunit E	1	1	1	hdrE
K14127	F420-non-reducing hydrogenase iron-sulfur subunit	2	1	0	mvhD
K04480	methanol—5-hydroxybenzimidazolylcobamide Co-methyltransferase	1	1	1	mtaB
K14080	[methyl-Co(III) methanol/glycine betaine-specific corrinoid protein]:coenzyme M methyltransferase	0	2	2	mtaA
K14081	methanol corrinoid protein	1	2	1	mtaC

To reduce methanol to methane, there are 6 main genes involved: mtaA, mtaB, mtaC and mcrABG (de Mesquita et al., 2023; Fischer et al., 2021). All of these six genes were identified in *Methanolobus* NM.31.1B and *Methanococcoides* M.31.2A, while all genes except mtaA were identified in *Methanococcoides* NM.31.1A.

The length of the genes varied between MAGs. All MAGs contained mcrABG, methyl-coenzyme M reductase (α, β and γ subunits). They were found in one copy in each MAG. The nucleotide length of subunit α varied between 1562 bases for *Methanococcoides* M.31.2A and 1718 bases for *Methanolobus* NM.31.1B and *Methanococcoides* NM.31.1A. Subunit β had the same length in all MAGs and subunit γ had the same length in *Methanococcoides* NM.31.1A and *Methanococcoides* M.31.2A (746 bases), and 3 additional bases in *Methanolobus* NM.31.1B (749 bases).

When methanol is reduced to methane, the heterodisulfide complex CoM-S-S-CoB is formed. This has to be split into CoM-SH and CoB-SH before a new methanol molecule can be reduced (Fischer et al., 2021). This reduction is catalysed by the enzyme heterodisulfide reductase (hdr). Hdr can either be in the membrane bound form hdrDE or in the cytoplasmic form hdrABC (Buan & Metcalf, 2010).

Methanolobus NM.31.1B contained genes for hdrDE, two copies of all subunits of hdrABC, as well as subunit mvhD from mvhAGD. MvhAGD forms a complex with hdrABC that together catalyse the CoM-S-S-CoB reduction (Kaster et al., 2011). HdrA or hdrB was not identified by DRAM in either *Methanococcoides* M.31.2A or *Methanococcoides* NM.31.1A. HdrDE was detected in both *Methanococcoides* MAGs. *Methanococcoides* M.31.2A also lacked the gene mvhD.

Methylotrophic methanogenesis by methyl dismutation is dependent on electrons obtained from the methyl branch of the Wood-Ljungdahl pathway (de Mesquita et al., 2023). The DRAM output was investigated for presence of the methyl branch of the Wood-Ljungdahl pathway. At most, three genes from the Wood-Ljungdahl pathway was found in either MAG. Methanogenesis by methyl reduction is dependent on obtaining electrons from H_2, formate or ethanol. The gene for formate dehydrogenase (fpo) subunit β was only found in *Methanolobus* NM.31.1B. Formate dehydrogenase is an enzyme that will oxidise formate to CO_2 (Park et al., 2024). No other MAGs had this gene.

4 Discussion

4.1 *Methanosarcinaceae* was enriched in the presence of methanol

Methanol seemed to be a significant factor for the enrichment of the methylotrophic methanogens. There was a significant increase of methanogenic archaea after two weeks in the sediment enrichment amended with methanol and with a slight delay in the corresponding enrichment amended with nitrate and methanol. The relative abundance increased from approximately 0 to 0.15 by the end of the incubation for both the mentioned enrichments. The same increase in relative abundance was not observed for the sediment enrichment amended with nitrate, or in the control enrichment.

Previous studies have investigated the abundance of methanogens in a variety of environments such as landfills, sewage treatment plants, wetlands (freshwater and coastal), rice fields, ocean sediment and more (de Mesquita et al., 2023). In almost all of these environments, *Methanosarcinaceae* was the most abundant methanogenic family. The same was noticed in the current experiment, where the only methanogenic family annotated among the top ten families was *Methanosarcinaceae.*

Methanosarcinaceae was one of the main differentially abundant families in both enrichments containing methanol. The relative abundance of *Methanosarcinaceae* increased significantly in the enrichments amended with methanol but not in the enrichments amended with nitrate. Therefore, it seems like methanol was a significant contributor for the enrichment of *Methanosarcinaceae*. The PCoA analysis indicate that methanol is the main explanatory factor for the variance between the different enrichments. The inferred functional groups from FAPROTAX also indicated an increase of organisms performing methylotrophic methanogenesis in both enrichments containing methanol.

Prior to the 16S rRNA amplicon sequencing analysis, the 16S rRNA gene was quantified using qPCR with *Methanolobus*-specific primers. An increase in N_0 was detected when *Methanolobus* primers were used in the sediment enrichments amended with methanol. This is an indication towards the increase in abundance of organisms within the genus *Methanolobus*, and perhaps also the family *Methanosarcinaceae*. The increase in N_0 happened simultaneously as where the increase of methanogens was detected in figure 3.4 and 3.5.

4.2 Methanogenic archaea were enriched at higher redox potential than expected from literature

From current knowledge, methanogenesis happens at redox potentials between -200 and -400 mV (Hirano et al., 2013; Vongvichiankul et al., 2017). To the author's knowledge, there is little data available on the effect of redox potential on methanogenesis in marine sediments. In the current experiment a significant increase in the relative abundance of *Methanosarcinaceae* was observed at redox potentials higher than what would be expected based on literature. When the initial increase of *Methanosarcinaceae* in the methanol enrichment was detected at day 17, the ORP was around +30 mV. From day 17 and to the end of the incubation, the ORP rose to approximately +100 mV.

For the sediment enrichment amended with nitrate and methanol, there was a significant increase in the relative abundance of *Methanosarcinaceae* from day 21. At this point, the ORP was -55 mV and +69 mV for the parallels. The ORP remained lower than for the sediment enrichment amended with methanol, but still higher than -200 mV for the rest of the incubation.

Some studies have tried to investigate the methanogenic capabilities of methanogens under varying redox potentials by changing the ORP manually. Attempts to increase the redox potential for hydrogenotrophic methanogenesis showed supressed CH_4 production for ORPs above -100 mV (Hirano et al., 2013). Methylotrophic methanogenesis have been found to have a threshold at +50 mV. *Methanosarcina barkeri* could decrease a positive redox potential created by ferricyanide to +50 mV and then initiate production of CH_4 (Fetzer & Conrad, 1993). Another study found that methylotrophic methanogens have a higher resistance to high redox conditions compared to acetoclastic methanogens. If the ORP is high, the methane production decreases over a longer time period than for hydrogenotrophic or acetoclastic methanogenesis (Shcherbakova et al., 1997).

The observations in the current experiment does not coincide with what has been found in literature. The measurements of ORP were performed on the surface of the sediments. It might be that if the measurements had been conducted further down into the sediments, that the ORP measurements would have been different.

Positive ORP values indicate an oxidizing environment, while negative ORP values indicate a reducing environment, and methanogenesis is a reducing process performed in anoxic conditions with low reduction potentials (Zobell, 1946). In figure 3.5 the relative abundance of *Methanosarcinaceae* is still increasing at day 31 for the sediment enrichments amended with

methanol. The incubation of the microcosms was concluded when the redox potential within the sediment enrichment amended with methanol consistently exceeded levels typically associated with methanogenesis, based on what is seen in literature (Fetzer & Conrad, 1993; Hirano et al., 2013; Vongvichiankul et al., 2017). For future research, extending the incubation beyond day 31 could have given insight into whether the relative abundances of *Methanosarcinaceae* would have continued increasing, at continuously rising redox potentials.

4.3 Potential inhibition of methanogenesis by ammonia

There appears to be a trend in the two sediment enrichments amended with methanol in which the increase of methanogenic archaea is not detected until ammonia concentrations have dropped below a crucial threshold. The synthetic seawater contained 0.2 mM ammonia, which is lower than inhibitory concentrations found in literature (Chen et al., 2008; Finn et al., 2023). In the sediment enrichment amended with methanol, the ammonia concentration decreases the fastest and correspondingly, the increase in relative abundance of methanogens is seen earlier than in the other enrichments. In the sediment enrichment amended with both nitrate and methanol the increase in relative abundance of *Methanosarcinaceae* is delayed by 4 days compared to the samples enriched with only methanol. The increase in abundance of *Methanosarcinaceae* was detected when ammonia levels reached a threshold of approximately 0.09 mM.

Methanogenesis can be influenced by ammonia due to its possible impacts on several cellular processes. Ammonia can permeate into the cells and affect intracellular pH, potassium concentration and cause osmotic stress (Yan et al., 2020). High ammonia concentrations have been shown to inhibit acetoclastic methanogenesis in bioreactors at thermophilic temperatures (Yang et al., 2018). Another study found that ammonia concentrations above 1.7 g/L are inhibitory for methane production (Chen et al., 2008).

Whether the ammonia is the reason for the delayed increase in relative abundance of *Methanosarcinaceae* in the sediment enrichments amended with nitrate and methanol is difficult to accurately assess. The other difference in these two enrichments that could be explanatory for the delay is the addition of nitrate. However, the nitrate concentrations do not exhibit a similar trend as the ammonia does. Since the nitrogen measurements were performed in the liquid media, it is difficult to conclude whether the measurements actually are representative for the chemistry in the sediments.

4.4 Methanol oxidisers might also utilise methanol

Previous research on the metabolism of methylotrophic compounds in marine sediments, particularly methanol, discovered that methanol is primarily oxidised to CO_2 (through sulfate reduction) with only a fraction undergoing methanogenesis (King et al., 1983).

From both the differential and relative abundances, the family *Piscirickettsiaceae* exhibited a significant increase in both sediment enrichments amended with methanol alongside *Methanosarcinaceae*. Within the family *Piscirickettsiaceae*, is the genus *Methylophaga* which is a known methanol oxidiser (Marshall et al., 2014).

The FAPROTAX analysis (figure 3.6) indicate a low abundance of methanol oxidising microorganisms. It was discovered that the family *Piscirickettsiaceae* was not represented in the FAPROTAX database, only the genus *Methylophaga*. Analysis of the genus composition in the sediments also indicate that a large portion of the phylum *Proteobacteria*, which include the family *Piscirickettsiaceae*, remain unclassified at genus level (figure A3). These discoveries indicate an underestimation of the abundance of methanol oxidising bacteria in the sediments.

Methylophaga can also perform dissimilatory reduction of nitrate to nitrite (Auclair et al., 2010). This reduction of nitrate to nitrite could also have contributed to the peak in nitrite accumulation in the two enrichments amended with nitrate (figure 3.2).

4.5 Possible pathways for methylotrophic methanogenesis

The metagenome analysis indicated that methyl reduction was the main methylotrophic pathway utilised by the methanogens in the sediment enrichments amended with methanol. Nearly all genes required for methyl reduction were identified in the MAGs. In contrast, methyl dismutation was considered a less probable pathway for the enriched methanogens. To consider methyl dismutation as feasible, the methyl branch of the Wood-Ljungdahl pathway should be present in the genome (Thauer et al., 2008). The DRAM output was consequently analysed for presence of genes belonging to the methyl branch of the Wood-Ljungdahl pathway. At most, three genes from the Wood-Ljungdahl pathway were found in a single MAG. Based on the information from literature, these three genes cannot be assumed to encompass the entire methyl branch of the Wood-Ljungdahl pathway (Kurth et al., 2020). This indicates that methyl reduction is more likely happening as a hydrogen dependent methanogenesis rather than methyl dismutation. However, the MAGs may not be true representations of the original genomes.

Methanolobus NM.31.1B contained the gene for formate dehydrogenase subunit β and might therefore be able to utilise formate as an electron donor. Methyl reduction is dependent on H_2,

which can come from electron donors such as formate or ethanol (Kurth et al., 2020). To utilise formate as an electron donor, the enzyme formate dehydrogenase is needed (Mota et al., 2011). Formate dehydrogenases catalyse the oxidation of the formate anion to carbon dioxide in a redox reaction that involves the transfer of two electrons from the substrate to the active site. This suggests that *Methanolobus* NM.31.1B might be able use formate as an electron donor for the reduction of methanol. Since formate dehydrogenase was not detected in the other MAGs, it is possible that these organisms use different electron donors.

From the inferred metabolisms in the FAPROTAX analysis (figure 3.6), "methanogenesis by disproportionation of methyl groups" (methyl dismutation) was more relative abundant than "methanogenesis by reduction of methyl compounds with H_2" (methyl reduction). This contradicts the genetic potential inferred from the MAGs. The discrepancy observed suggests that there might be a higher presence of methyl dismutation in the database compared to methyl reduction, potentially skewing the output from the analysis.

The FAPROTAX analysis is based on inferred metabolisms from the taxonomic annotation from the 16S rRNA amplicon analysis. The metagenome data on the other hand is more reliable because it only is dependent on software finding the reading frames in the MAGs and from there identify the gene.

4.6 Methanogenesis from methylamines

While methanol is the most likely substrate utilised by the methanogens in the current enrichment experiment, it is possible that methanogenesis from methylamines is performed *in situ*. All archaeal MAGs contained genes for conversion of trimethylamine to methyl-CoM, and *Methanococcoides* NM.31.1A and *Methanococcoides* M.31.2A also contained the genes for conversion of methylamine into methyl-CoM.

Neither *Methanococcoides* nor *Methanolobus* have been demonstrated to metabolise acetate or H_2/CO_2 to methane (Boone et al., 2001; Liang et al., 2022). *Methanolobus* have not been shown to perform acetoclastic or hydrogenotrophic methanogenesis, only methylotrophic, and form methane from methanol and methylated amines without external H_2 – meaning that they can perform methyl dismutation. However, the genetic potential inferred from *Methanolobus* NM.31.1B did not align with this information. *Methanolobus* NM.31.1B might have the genetic potential to utilise formate as an electron donor for the reduction of methanol through methyl reduction as formate dehydrogenase was located in the MAG.

Methanococcoides can as far as we know only grow using methylated compounds as substrate, and it is uncertain whether it can perform methyl reduction, methyl dismutation or both (Liang et al., 2022). The genetic potential inferred from *Methanococcoides* M.31.2A and *Methanococcoides* NM.31.1A indicated only methyl reduction, and not methyl dismutation. Further studies are needed to elucidate the specific methane production pathways in these microorganisms.

4.7 Methanogens are obligate methane producers

No tests were conducted to investigate whether the increase in relative abundance of *Methanosarcinaceae* corresponded to an increase in CH_4 production. Such an analysis would require measuring CH_4 production in the microcosms. Furthermore, the genetic analyses also give no indication as to whether the genes were actually expressed in the cells. As no proteomic or transcriptomic analyses were conducted, the information is solely based on genetic potential.

Although methylotrophic methanogens were detected with sequencing-based methods, methane production was not confirmed by chemical assays. All known methanogens are obligate methane producers and they do not have other known metabolisms to generate energy (Buan, 2018). The standard free energy change for methylotrophic methanogenesis is between -49 and -113 kJ/mol, but also varies greatly depending on the H_2 concentration in the environment (Lyu et al., 2018). This suggests that the enrichment of the methanogenic archaea observed in the current thesis likely corresponds to an increase in methanogenesis even though methane production was not directly measured.

4.8 Technical limitations

4.8.1 DRAM only annotated two types of methylotrophic methanogenesis

Methylotrophic methanogenesis encompasses the utilisation of several substrates, some of which are listed in table 1.1. Following the DRAM annotation of the three MAGs the only output related to methylotrophic methanogenesis was methanogenesis from methanol and methylamines. When looking at metabolic pathways in KEGG, methanol and methylamines were also the only substrates identified. Since the focus of the present study was to enrich marine methanogenic archaea through methanol utilisation, investigations into other substrates were of relatively low significance. If later studies aim to enrich methanogenic archaea using other substrates than methanol or methylamines, these metabolisms need to be explored further.

4.8.2 The genome size of the MAGs did not correspond with literature

There was observed a large difference in the genome size and the number of genes within each MAG. *Methanolobus* NM.31.1B had the smallest genome of 2.14 Mbp, which was almost half the size of the two other archaeal MAGs. On the other hand, *Methanolobus* NM.31.1B had the highest number of annotated methanogenesis genes of all MAGs at 105.

The average genome size for complete *Methanolobus* genomes on NCBI[8] is approximately 3.00 Mbp, nearly 30 % larger than what was observed from the DRAM output. In contrast, the genome sizes for the *Methanococcoides* MAGs were 4.45 and 3.45 Mbp. Complete genomes for *Methanococcoides* on NCBI[9] have an average complete genome size of 2.48, indicating a discrepancy between the shotgun data and existing genome data. The differences in genome sizes could stem from various factors such as sequencing quality, a large amount of repeat regions in the genomes sequenced or low read overlap in the data (Sharpton, 2014).

4.8.3 Chemical measurements

When the experiment was set up, 0.1 % methanol was added to the sediment amended with methanol enriched media. However, the subsequent methanol concentration is not known. An attempt was made to adapt a practical colorimetric method for monitoring methanol during the incubation period. Unfortunately, the method tested was unsuccessful. If the methanol concentration had been possible to monitor, it would have enabled observation of conversion rates in the media.

When conducting the different chemical assays for measuring nitrate, nitrite, and ammonia concentrations, a single standard and blank were measured while liquid samples from the enrichment experiment were measured in triplicate.

The nitrate assay was the one that involved the most reagents. Reagent B had high viscosity, making accurate pipetting difficult. Due to this it was also very important to mix the samples well on a vortex before incubation. Additionally, the standard sample often did not measure as expected. This necessitated the making of new stocks of KNO_3, and of the different reagents. This led to the creation of 4 different standard curves (figure A4 to A7) for the nitrate assay which were utilised at different time points in the incubation period.

[8] https://www.ncbi.nlm.nih.gov/datasets/genome/?taxon=2220 accessed 17.04.2024
[9] https://www.ncbi.nlm.nih.gov/datasets/genome/?taxon=2225 accessed 17.04.2024

The variations observed, particularly within the nitrate assay, suggests that the variability might be more of a technical nature than true differences in concentrations. This underscores the importance of proper validation of chemical protocols, to ensure accurate and reliable measurements in future experiments.

4.9 Future aspects

In the current experiment, the metagenomic analysis only assessed genes directly involved in reducing methanol to methane. The processes and pathways behind methanogenesis are much more complex than what is given impression of in this thesis. About 200 genes are necessary to encode the biosynthesis of the coenzymes and enzyme systems required for methanogenesis (Lyu et al., 2018). Future interesting aspects would be to investigate the actual presence of methanogenesis through the analysis of production of CH_4 as well as studies on which methylotrophic pathways are utilised by the methanogens. Monitoring of the ORP would also propose interesting aspects, to see if the high redox potential can be recreated. Longer incubation time of the microcosms and the use of more specific archaeal primers would also give more insight to this field of study.

4.10 Conclusion

In conclusion the enrichments were successful in the sense that methanogenic archaea significantly rose in relative abundance from the beginning to the end of the incubation. In addition, the shotgun metagenomic analysis allowed for investigations into the genetic potential behind methylotrophic methanogenesis. However, a remaining question is how methylotrophic methanogenesis can have occurred at ORPs above +50 and +100 mV. This poses an interesting theme for future research.

References

Aguilar-Torrejón, J. A., Balderas-Hernández, P., Roa-Morales, G., Barrera-Díaz, C. E., Rodríguez-Torres, I., & Torres-Blancas, T. (2023). Relationship, importance, and development of analytical techniques: COD, BOD, and, TOC in water-An overview through time. *Sn Applied Sciences*, *5*(4). https://doi.org/10.1007/s42452-023-05318-7

Akinnawo, S. O. (2023). Eutrophication: Causes, consequences, physical, chemical and biological techniques for mitigation strategies. *Environmental Challenges*, *12*, 100733. https://doi.org/10.1016/j.envc.2023.100733

Allen, M. A., Lauro, F. M., Williams, T. J., Burg, D., Siddiqui, K. S., De Francisci, D., Chong, K. W. Y., Pilak, O., Chew, H. H., De Maere, M. Z., Ting, L., Katrib, M., Ng, C., Sowers, K. R., Galperin, M. Y., Anderson, I. J., Ivanova, N., Dalin, E., Martinez, M., . . . Cavicchioli, R. (2009). The genome sequence of the psychrophilic archaeon, *Methanococcoides burtonii*: the role of genome evolution in cold adaptation. *Isme Journal*, *3*(9), 1012-1035. https://doi.org/10.1038/ismej.2009.45

Amon, R. M. W., & Benner, R. (1996). Bacterial utilization of different size classes of dissolved organic matter. *Limnology and Oceanography*, *41*(1), 41-51. https://doi.org/10.4319/lo.1996.41.1.0041

Anthony, C. (1975). The biochemistry of methylotrophic micro-organisms. *Science Progress (1933-)*, *62*(246), 167-206. http://www.jstor.org/stable/43420299

Auclair, J., Lépine, F., Parent, S., & Villemur, R. (2010). Dissimilatory reduction of nitrate in seawater by a *Methylophaga* strain containing two highly divergent *narG* sequences. *Isme Journal*, *4*(10), 1302-1313. https://doi.org/10.1038/ismej.2010.47

Benjamini, Y., & Hochberg, Y. (1995). Controlling the False Discovery Rate: A Practical and Powerful Approach to Multiple Testing. *Journal of the Royal Statistical Society. Series B (Methodological)*, *57*(1), 289-300. http://www.jstor.org/stable/2346101

Boone, D. R., Castenholz, R. W., Garrity, G. M., & Bergey, D. H. (2001). *Bergey's manual of systematic bacteriology : Vol. 1 : The archaea and the deeply branching and phototrophic bacteria* (2nd ed., Vol. Vol. 1). Springer.

Bruice, P., Y. (2016). *Essential Organic Chemistry* (Third edition ed.). Pearson Education.

Buan, N. R. (2018). Methanogens: pushing the boundaries of biology. *Emerging Topics in Life Sciences*, *2*(4), 629-646. https://doi.org/10.1042/ETLS20180031

Buan, N. R., & Metcalf, W. W. (2010). Methanogenesis by *Methanosarcina acetivorans* involves two structurally and functionally distinct classes of heterodisulfide reductase. *Molecular Microbiology*, *75*(4), 843-853. https://doi.org/10.1111/j.1365-2958.2009.06990.x

Bushnell, B., Rood, J., & Singer, E. (2017). BBMerge - Accurate paired shotgun read merging via overlap. *PLoS One*, *12*(10). https://doi.org/10.1371/journal.pone.0185056

Chaumeil, P. A., Mussig, A. J., Hugenholtz, P., & Parks, D. H. (2020). GTDB-Tk: a toolkit to classify genomes with the Genome Taxonomy Database. *Bioinformatics*, *36*(6), 1925-1927. https://doi.org/10.1093/bioinformatics/btz848

Chavez, F. P., Messié, M., & Pennington, J. T. (2011). Marine Primary Production in Relation to Climate Variability and Change. *Annual Review of Marine Science, Vol 3*, *3*, 227-260. https://doi.org/10.1146/annurev.marine.010908.163917

Chen, K., & Pachter, L. (2005). Bioinformatics for whole-genome shotgun sequencing of microbial communities. *Plos Computational Biology*, *1*(2), 106-112. https://doi.org/10.1371/journal.pcbi.0010024

Chen, Y., Cheng, J. J., & Creamer, K. S. (2008). Inhibition of anaerobic digestion process: A review. *Bioresource Technology*, *99*(10), 4044-4064. https://doi.org/10.1016/j.biortech.2007.01.057

Chklovski, A., Parks, D. H., Woodcroft, B. J., & Tyson, G. W. (2023). CheckM2: a rapid, scalable and accurate tool for assessing microbial genome quality using machine learning. *Nature Methods*, *20*(8), 1203-1212. https://doi.org/10.1038/s41592-023-01940-w

Conrad, R. (2020). Importance of hydrogenotrophic, aceticlastic and methylotrophic methanogenesis for methane production in terrestrial, aquatic and other anoxic environments: A mini review. *Pedosphere*, *30*(1), 25-39. https://doi.org/10.1016/S1002-0160(18)60052-9

de Mesquita, C. P. B., Wu, D. Y., & Tringe, S. G. (2023). Methyl-Based Methanogenesis: an Ecological and Genomic Review. *Microbiology and Molecular Biology Reviews*, *87*(1). https://doi.org/10.1128/mmbr.00024-22

de Vries, W. (2021). Impacts of nitrogen emissions on ecosystems and human health: A mini review. *Current Opinion in Environmental Science & Health*, *21*. https://doi.org/10.1016/j.coesh.2021.100249

De Vrieze, J., Hennebel, T., Boon, N., & Verstraete, W. (2012). *Methanosarcina*: The rediscovered methanogen for heavy duty biomethanation. *Bioresource Technology*, *112*, 1-9. https://doi.org/10.1016/j.biortech.2012.02.079

Dziewit, L., Pyzik, A., Romaniuk, K., Sobczak, A., Szczesny, P., Lipinski, L., Bartosik, D., & Drewniak, L. (2015). Novel molecular markers for the detection of methanogens and phylogenetic analyses of methanogenic communities. *Frontiers in Microbiology*, *6*. https://doi.org/10.3389/fmicb.2015.00694

Fetzer, S., & Conrad, R. (1993). Effect of redox potential on methanogenesis by *Methanosarcina barkeri*. *Archives of Microbiology*, *160*(2), 108-113. https://doi.org/10.1007/BF00288711

Finn, D. R., Rohe, L., Krause, S., Guliyev, J., Loewen, A., & Tebbe, C. C. (2023). Methanogenesis in biogas reactors under inhibitory ammonia concentration requires community-wide tolerance. *Applied Microbiology and Biotechnology*, *107*(21), 6717-6730. https://doi.org/10.1007/s00253-023-12752-5

Fischer, P. Q., Sánchez-Andrea, I., Stams, A. J. M., Villanueva, L., & Sousa, D. Z. (2021). Anaerobic microbial methanol conversion in marine sediments. *Environmental Microbiology*, *23*(3), 1348-1362. https://doi.org/10.1111/1462-2920.15434

Forurensningsforskriften. (2004). *Forskrift om begrensning av forurensning*. (FOR-2004-06-01-931). Retrieved from https://lovdata.no/lov/1981-03-13-6

Galloway, J. N., Schlesinger, W. H., Levy, H., Michaels, A., & Schnoor, J. L. (1995). Nitrogen-Fixation - Anthropogenic Enhancement-Environmental Response. *Global Biogeochemical Cycles*, *9*(2), 235-252. https://doi.org/10.1029/95gb00158

Gan, Y., Meng, X., Gao, C., Song, W., Liu, L., & Chen, X. (2023). Metabolic engineering strategies for microbial utilization of methanol. *Engineering Microbiology*, *3*(3), 100081. https://doi.org/10.1016/j.engmic.2023.100081

Gao, K. S., Helbling, E. W., Häder, D. P., & Hutchins, D. A. (2012). Responses of marine primary producers to interactions between ocean acidification, solar radiation, and warming. *Marine Ecology Progress Series*, *470*, 167-189. https://doi.org/10.3354/meps10043

Garcia, J. L., Patel, B. K. C., & Ollivier, B. (2000). Taxonomic phylogenetic and ecological diversity of methanogenic *Archaea*. *Anaerobe*, *6*(4), 205-226. https://doi.org/10.1006/anae.2000.0345

Gruber, N., Boyd, P. W., Frölicher, T. L., & Vogt, M. (2021). Biogeochemical extremes and compound events in the ocean. *Nature*, *600*(7889), 395-407. https://doi.org/10.1038/s41586-021-03981-7

Hallegraeff, G. M. (1993). A Review of Harmful Algal Blooms and Their Apparent Global Increase. *Phycologia*, *32*(2), 79-99. https://doi.org/10.2216/i0031-8884-32-2-79.1
Hirano, S., Matsumoto, N., Morita, M., Sasaki, K., & Ohmura, N. (2013). Electrochemical control of redox potential affects methanogenesis of the hydrogenotrophic methanogen *Methanothermobacter thermautotrophicus*. *Letters in Applied Microbiology*, *56*(5), 315-321. https://doi.org/10.1111/lam.12059
Hutchins, D. A., & Capone, D. C. (2022). The marine nitrogen cycle: new developments and global change. *Nature Reviews Microbiology*, *20*(7), 401-414. https://doi.org/10.1038/s41579-022-00687-z
Johansen, T. A. (2001). *Under byens gater: Oslos vann- og avløpshistorie*. Oslo kommune, Vann- og avløpsetaten.
Johnson, J. S., Spakowicz, D. J., Hong, B. Y., Petersen, L. M., Demkowicz, P., Chen, L., Leopold, S. R., Hanson, B. M., Agresta, H. O., Gerstein, M., Sodergren, E., & Weinstock, G. M. (2019). Evaluation of 16S rRNA gene sequencing for species and strain-level microbiome analysis. *Nature Communications*, *10*. https://doi.org/10.1038/s41467-019-13036-1
Kang, D. W. D., Li, F., Kirton, E., Thomas, A., Egan, R., An, H., & Wang, Z. (2019). MetaBAT 2: an adaptive binning algorithm for robust and efficient genome reconstruction from metagenome assemblies. *PeerJ*, *7*. https://doi.org/10.7717/peerj.7359
Kaster, A. K., Moll, J., Parey, K., & Thauer, R. K. (2011). Coupling of ferredoxin and heterodisulfide reduction via electron bifurcation in hydrogenotrophic methanogenic archaea. *Proceedings of the National Academy of Sciences of the United States of America*, *108*(7), 2981-2986. https://doi.org/10.1073/pnas.1016761108
King, G. M., Klug, M. J., & Lovley, D. R. (1983). Metabolism of Acetate, Methanol, and Methylated Amines in Intertidal Sediments of Lowes Cove, Maine. *Applied and Environmental Microbiology*, *45*(6), 1848-1853. https://doi.org/10.1128/Aem.45.6.1848-1853.1983
Klüber, H. D., & Conrad, R. (1998). Effects of nitrate, nitrite, NO and N_2O on methanogenesis and other redox processes in anoxic rice field soil. *Fems Microbiology Ecology*, *25*(3), 301-318. https://doi.org/10.1016/S0168-6496(98)00011-7
Kurth, J. M., op den Camp, H. J. M., & Welte, C. U. (2020). Several ways one goal-methanogenesis from unconventional substrates. *Applied Microbiology and Biotechnology*, *104*(16), 6839-6854. https://doi.org/10.1007/s00253-020-10724-7
Landrigan, P. J., Stegeman, J. J., Fleming, L. E., Allemand, D., Anderson, D. M., Backer, L. C., Brucker-Davis, F., Chevalier, N., Corra, L., Czerucka, D., Bottein, M. Y. D., Demeneix, B., Depledge, M., Deheyn, D. D., Dorman, C. J., Fénichel, P., Fisher, S., Gaill, F., Galgani, F., . . . Rampal, P. (2020). Human Health and Ocean Pollution. *Annals of Global Health*, *86*(1). https://doi.org/10.5334/aogh.2831
Laudadio, I., Fulci, V., Palone, F., Stronati, L., Cucchiara, S., & Carissimi, C. (2018). Quantitative Assessment of Shotgun Metagenomics and 16S rDNA Amplicon Sequencing in the Study of Human Gut Microbiome. *Omics-a Journal of Integrative Biology*, *22*(4), 248-254. https://doi.org/10.1089/omi.2018.0013
Liang, L. W., Sun, Y., Dong, Y. J., Ahmad, T., Chen, Y. F., Wang, J., & Wang, F. P. (2022). *Methanococcoides orientis* sp. nov., a methylotrophic methanogen isolated from sediment of the East China Sea. *International Journal of Systematic and Evolutionary Microbiology*, *72*(5). https://doi.org/10.1099/ijsem.0.005384

Louca, S., Parfrey, L. W., & Doebeli, M. (2016). Decoupling function and taxonomy in the global ocean microbiome. *Science*, *353*(6305), 1272-1277. https://doi.org/10.1126/science.aaf4507

Lyu, Z., & Liu, Y. (2019). Diversity and Taxonomy of Methanogens. In A. J. M. Stams & D. Z. Sousa (Eds.), *Biogenesis of Hydrocarbons* (pp. 19-77). Springer International Publishing. https://doi.org/10.1007/978-3-319-78108-2_5

Lyu, Z., Shao, N., Akinyemi, T., & Whitman, W. B. (2018). Methanogenesis. *Curr Biol*, *28*(13), R727-R732. https://doi.org/10.1016/j.cub.2018.05.021

Marshall, S. H., Gómez, F. A., & Klose, K. E. (2014). The Genus *Piscirickettsia*. In E. Rosenberg, E. F. DeLong, S. Lory, E. Stackebrandt, & F. Thompson (Eds.), *The Prokaryotes: Gammaproteobacteria* (pp. 565-573). Springer Berlin Heidelberg. https://doi.org/10.1007/978-3-642-38922-1_234

Martin, J. (2023). *Investigating the effects of methanol on ammonia-oxidising archaea in marine sediment microcosms* [Master of Science, Norwegian University of Life Sciences].

Martiny, J. B. H., Jones, S. E., Lennon, J. T., & Martiny, A. C. (2015). Microbiomes in light of traits: A phylogenetic perspective. *Science*, *350*(6261). https://doi.org/10.1126/science.aac9323

McGarvey, R., Dowling, N., & Cohen, J. E. (2016). Longer Food Chains in Pelagic Ecosystems: Trophic Energetics of Animal Body Size and Metabolic Efficiency. *Am Nat*, *188*(1), 76-86. https://doi.org/10.1086/686880

McMurdie, P. J., & Holmes, S. (2013). phyloseq: An R Package for Reproducible Interactive Analysis and Graphics of Microbiome Census Data. *PLoS One*, *8*(4). https://doi.org/10.1371/journal.pone.0061217

Mishra, S., Singh, V., Cheng, L., Hussain, A., & Ormeci, B. (2022). Nitrogen removal from wastewater: A comprehensive review of biological nitrogen removal processes, critical operation parameters and bioreactor design. *Journal of Environmental Chemical Engineering*, *10*(3). https://doi.org/10.1016/j.jece.2022.107387

Mota, C. S., Rivas, M. G., Brondino, C. D., Moura, I., Moura, J. J. G., González, P. J., & Cerqueira, N. M. F. S. A. (2011). The mechanism of formate oxidation by metal-dependent formate dehydrogenases. *Journal of Biological Inorganic Chemistry*, *16*(8), 1255-1268. https://doi.org/10.1007/s00775-011-0813-8

Nurk, S., Meleshko, D., Korobeynikov, A., & Pevzner, P. A. (2017). metaSPAdes: a new versatile metagenomic assembler. *Genome Research*, *27*(5), 824-834. https://doi.org/10.1101/gr.213959.116

Nyberg, U., Aspegren, H., Andersson, B., Jansen, J. L., & Villadsen, I. S. (1992). Full-Scale Application of Nitrogen Removal with Methanol as Carbon Source. *Water Science and Technology*, *26*(5-6), 1077-1086. https://doi.org/10.2166/wst.1992.0549

Olm, M. R., Brown, C. T., Brooks, B., & Banfield, J. F. (2017). dRep: a tool for fast and accurate genomic comparisons that enables improved genome recovery from metagenomes through de-replication. *Isme Journal*, *11*(12), 2864-2868. https://doi.org/10.1038/ismej.2017.126

Oremland, R. S., & Boone, D. R. (1994). *Methanolobus Taylorii* sp. nov., a New Methylotrophic, Estuarine Methanogen. *International Journal of Systematic Bacteriology*, *44*(3), 573-575. https://doi.org/10.1099/00207713-44-3-573

Oren, A. (2014). The Family *Methanosarcinaceae*. In E. Rosenberg, E. F. DeLong, S. Lory, E. Stackebrandt, & F. Thompson (Eds.), *The Prokaryotes: Other Major Lineages of Bacteria and The Archaea* (pp. 259-281). Springer Berlin Heidelberg. https://doi.org/10.1007/978-3-642-38954-2_408

Ott, J., Gronemann, V., Pontzen, F., Fiedler, E., Grossman, G., Kersebom, D. B., Weiss, G., & Witte, C. (2012). Methanol. In *Ullmann's Encyclopedia of Industrial Chemistry* (pp. 27). Wiley-VCH. https://doi.org/10.1002/14356007.a16_465.pub3

Oviatt, C., Doering, P., Nowicki, B., Reed, L., Cole, J., & Frithsen, J. (1995). An Ecosystem-Level Experiment on Nutrient Limitation in Temperate Coastal Marine Environments. *Marine Ecology Progress Series*, *116*(1-3), 171-179. https://doi.org/10.3354/meps116171

Park, J., Heo, Y., Jeon, B. W., Jung, M. Y., Kim, Y. H., Lee, H. H., & Roh, S. H. (2024). Structure of recombinant formate dehydrogenase from *Methylobacterium extorquens* (MeFDH1). *Scientific Reports*, *14*(1). https://doi.org/10.1038/s41598-024-54205-7

Pelaz, L., Gómez, A., Letona, A., Garralón, G., & Fdz-Polanco, M. (2018). Nitrogen removal in domestic wastewater. Effect of nitrate recycling and COD/N ratio. *Chemosphere*, *212*, 8-14. https://doi.org/10.1016/j.chemosphere.2018.08.052

R Core Team. (2024). *R: A Language and Environment for Statistical Computing*. In R Foundation for Statistical Computing. https://www.R-project.org/

Rognes, T., Flouri, T., Nichols, B., Quince, C., & Mahé, F. (2016). VSEARCH: a versatile open source tool for metagenomics. *PeerJ*, *4*. https://doi.org/10.7717/peerj.2584

Rojo, F. (2009). Degradation of alkanes by bacteria. *Environmental Microbiology*, *11*(10), 2477-2490. https://doi.org/10.1111/j.1462-2920.2009.01948.x

Ruijter, J. M., Ramakers, C., Hoogaars, W. M. H., Karlen, Y., Bakker, O., van den Hoff, M. J. B., & Moorman, A. F. M. (2009). Amplification efficiency: linking baseline and bias in the analysis of quantitative PCR data. *Nucleic Acids Research*, *37*(6). https://doi.org/10.1093/nar/gkp045

Ruiz-Villalba, A., Ruijter, J. M., & van den Hoff, M. J. B. (2021). Use and Misuse of C_q in qPCR Data Analysis and Reporting. *Life-Basel*, *11*(6). https://doi.org/10.3390/life11060496

SALT, NINA, NIVA, Havforskningsinstituttet. (2019). *Kunnskapsstatus Oslofjorden*. https://www.miljodirektoratet.no/globalassets/publikasjoner/m1556/m1556.pdf

Shaffer, M., Borton, M. A., McGivern, B. B., Zayed, A. A., La Rosa, S. L., Solden, L. M., Liu, P. F., Narrowe, A. B., Rodriguez-Ramos, J., Bolduc, B., Gazitua, M. C., Daly, R. A., Smith, G. J., Vik, D. R., Pope, P. B., Sullivan, M. B., Roux, S., & Wrighton, K. C. (2020). DRAM for distilling microbial metabolism to automate the curation of microbiome function. *Nucleic Acids Research*, *48*(16), 8883-8900. https://doi.org/10.1093/nar/gkaa621

Sharpton, T. J. (2014). An introduction to the analysis of shotgun metagenomic data. *Frontiers in Plant Science*, *5*. https://doi.org/10.3389/fpls.2014.00209

Shcherbakova, V., Laurinavichius, K., Obraztsova, A. Y., & Akimenko, V. K. (1997). The effect of redox potential on methanogenesis by thermophilic methanogens. *Microbiology*, *66*, 642-646.

Sonune, A., & Ghate, R. (2004). Developments in wastewater treatment methods. *Desalination*, *167*(1-3), 55-63. https://doi.org/10.1016/j.desal.2004.06.113

Stoddard, S. F., Smith, B. J., Hein, R., Roller, B. R. K., & Schmidt, T. M. (2015). *rrnDB*: improved tools for interpreting rRNA gene abundance in bacteria and archaea and a new foundation for future development. *Nucleic Acids Research*, *43*(D1), D593-D598. https://doi.org/10.1093/nar/gku1201

Thakur, I. S., & Medhi, K. (2019). Nitrification and denitrification processes for mitigation of nitrous oxide from waste water treatment plants for biovalorization: Challenges and opportunities. *Bioresource Technology*, *282*, 502-513. https://doi.org/10.1016/j.biortech.2019.03.069

Thauer, R. K., Kaster, A. K., Seedorf, H., Buckel, W., & Hedderich, R. (2008). Methanogenic archaea: ecologically relevant differences in energy conservation. *Nature Reviews Microbiology*, *6*(8), 579-591. https://doi.org/10.1038/nrmicro1931

Vongvichiankul, C., Deebao, J., & Khongnakorn, W. (2017). Relationship between pH, Oxidation Reduction Potential (ORP) and Biogas Production in Mesophilic Screw Anaerobic Digester. *2017 International Conference on Alternative Energy in Developing Countries and Emerging Economies*, *138*, 877-882. https://doi.org/10.1016/j.egypro.2017.10.113

Wickham, H. (2016). *ggplot2 : elegant graphics for data analysis* (2nd edition. ed.). Springer International Publishingr.

Wu, Y. W., Simmons, B. A., & Singer, S. W. (2016). MaxBin 2.0: an automated binning algorithm to recover genomes from multiple metagenomic datasets. *Bioinformatics*, *32*(4), 605-607. https://doi.org/10.1093/bioinformatics/btv638

Yan, M., Treu, L., Zhu, X. Y., Tian, H. L., Basile, A., Fotidis, I. A., Campanaro, S., & Angelidaki, I. (2020). Insights into Ammonia Adaptation and Methanogenic Precursor Oxidation by Genome-Centric Analysis. *Environmental Science & Technology*, *54*(19), 12568-12582. https://doi.org/10.1021/acs.est.0c01945

Yang, Z. Y., Wang, W., He, Y. F., Zhang, R. H., & Liu, G. Q. (2018). Effect of ammonia on methane production, methanogenesis pathway, microbial community and reactor performance under mesophilic and thermophilic conditions. *Renewable Energy*, *125*, 915-925. https://doi.org/10.1016/j.renene.2018.03.032

Zobell, C. E. (1946). Studies on Redox Potential of Marine Sediments. *Aapg Bulletin-American Association of Petroleum Geologists*, *30*(4), 477-513. https://doi.org/10.1306/3d933808-16b1-11d7-8645000102c1865d

Appendix

Protocol for gel electrophoresis

In the current thesis, 1 %, 1.5 % and 2 % agarose gel electrophoresis was run. To make 50 ml 1 % gel, 0.5 g UltraPure™ agarose (Thermo Fisher Scientific, USA) was combined with 50 ml Tris base, acetic acid and EDTA buffer (TAE buffer). Correspondingly, gels with 1.5 % was made with 0.75 g agarose, and 2 % gels with 1 g agarose per 50 ml TAE buffer. The mixture was heated on maximum heat in a microwave to dissolve the agarose, trying to avoid boiling the mixture. When dissolved, PeqGREEN DNA/RNA dye (VWR, Germany) was added, 2 µl per 50 ml gel product.

A gel tray with combs was set up, and the gel was poured in. Any air bubbles were removed using a pipette tip. Once cool, after approximately 10-15 minutes, the comb was removed, and the gel transferred to a gel system containing TAE buffer. In the first well, 4 µl 100 bp DNA ladder RTL (Solis BioDyne, Estonia) was added, and to the other wells, 5 µl sample. If samples were Ready To Load, they were added directly to the gel, if not, they were added 1 µl 6 x loading dye (Solis BioDyne, Estonia) and mixed well first before loading on the gel. All gels were run at 80V between 30-50 minutes. After the gels were run, they were visualised by trans UV on a Gel Doc™ XR machine (Bio-Rad, USA).

qPCR results on the DNA extracted from the sediment samples

QPCR analysis was run on all extracted DNA from the sediment samples. Two runs were performed, one with bacterial short range 16S rRNA PRK primers, and one with *Methanolobus* primers. The LinReg transformed N_0-values can be seen in figure A1. The N_0 values were generally higher when using PRK primers compared to *Methanolobus* primers. In figure B the N_0-values can be seen having a steep increase in the methanol and the nitrate + methanol enrichments from approximately the halfway point of the incubation.

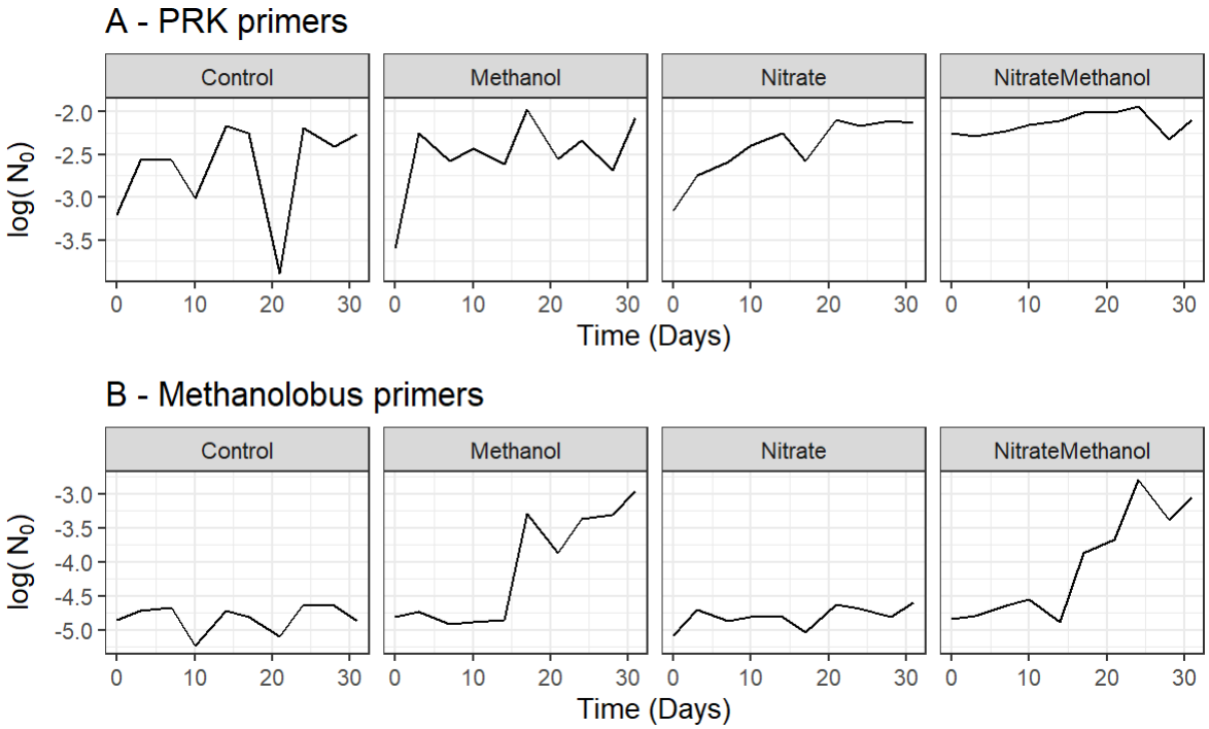

Figure A1: Log10 of all N_0-values from the two separate qPCR runs. Plot A is from the run using PRK primers, and plot B is from the run using *Methanolobus* primers.

Null sample abundance

A null sample was taken from the sediment before it was split into four different enrichments and covered with enriched media. Figure A2 show the taxonomic composition of the null sample at family level.

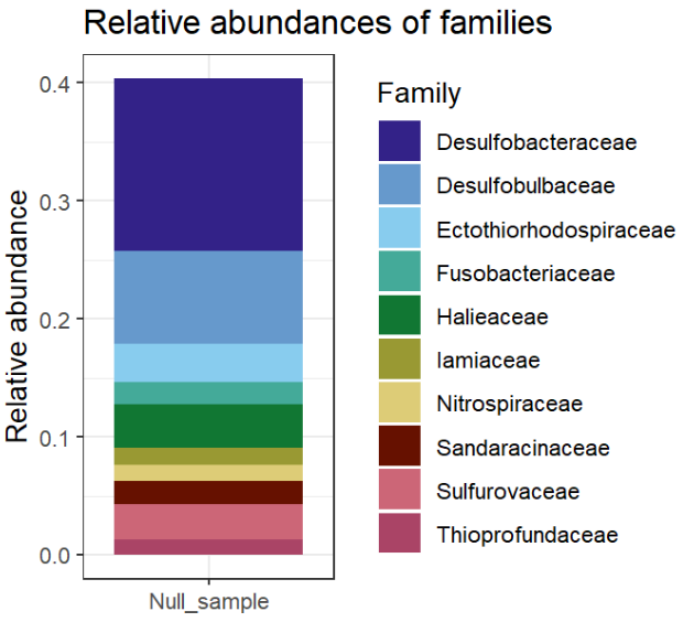

Figure A2: Taxonomic composition of the null sample of the sediment. The corresponding N_0 values from the qPCR analysis were -3.18 (PRK primers) and -5.78 (*Methanolobus* primers).

Classification on genus level

The OTUs in the samples were also classified to genus level. Since the standard procedure when making a phyloseq object is to only keep genera classification when the genus score from the taxonomic annotation is higher than 0.8, many genera are “unclassified”. To illustrate the taxonomic composition on genus level, all unclassified genera were given NA status in the phyloseq object. Therefore, the top classified OTUs are shown, and the rest are in the group “Other <phylum>”. This plot illustrates the proportion of unclassified genera within each phylum.

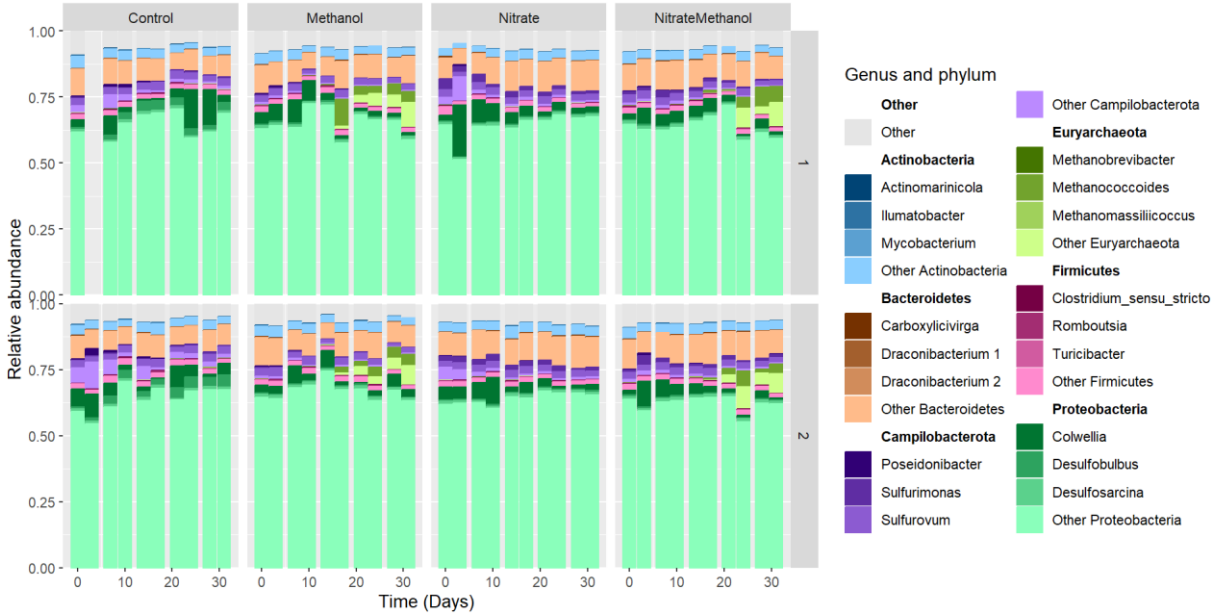

Figure A3: Taxonomic composition of the sediment samples on genus level. The two most relative abundant classified genera in each phylum are shown under each phylum name. All unclassified genera in each phylum are in the group “Other <phylum>”.

Standard curves

The standard measurements of nitrate were not consistent. The expected spectrophotometric values, based on the standard curves were often not observed. It was therefore determined that new standard curves had to be made each time the standard measurement deviated too much from the expected value. Therefore, there are 4 separate standard curves for nitrate.

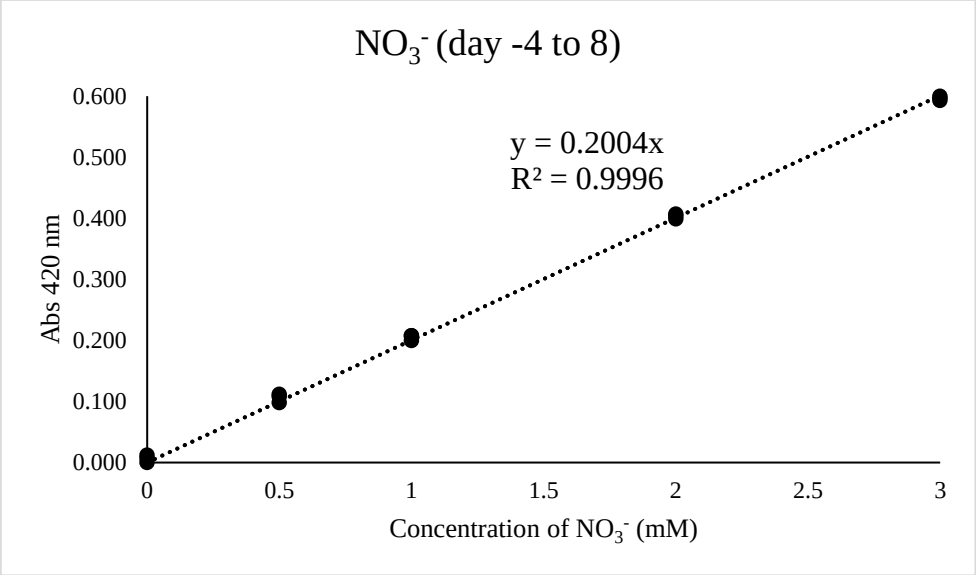

Figure A4: The first standard curve made for the NO_3^- measurements. It was used to calculate NO_3^- concentrations from day -4 to day 8.

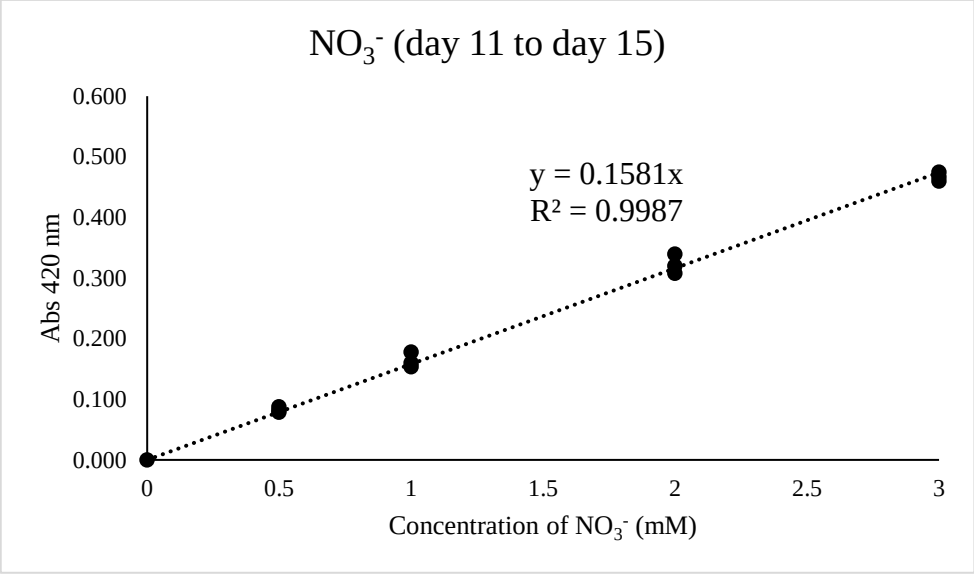

Figure A5: The second standard curve made for the NO_3^- measurements. It was used to calculate NO_3^- concentrations from day 11 to day 15.

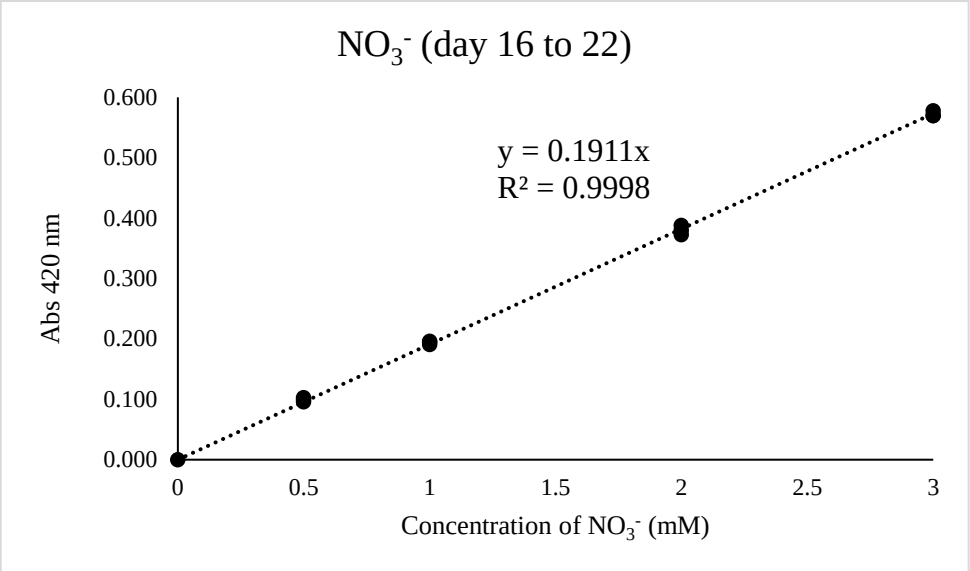

Figure A6: The third standard curve made for the NO_3^- measurements. It was used to calculate NO_3^- concentrations from day 16 to day 22.

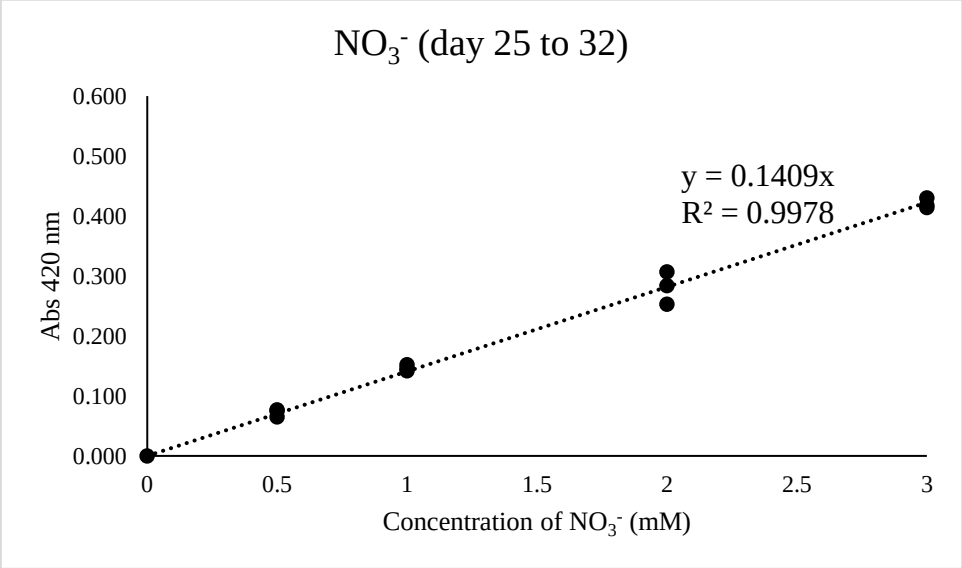

Figure A7: The fourth standard curve made for the NO_3^- measurements. It was used to calculate NO_3^- concentrations from day 25 to day 32.

The standard measurements for nitrite and ammonia did not deviate from the expected values from the standard sample, so the same standard curve was used throughout the entire incubation.

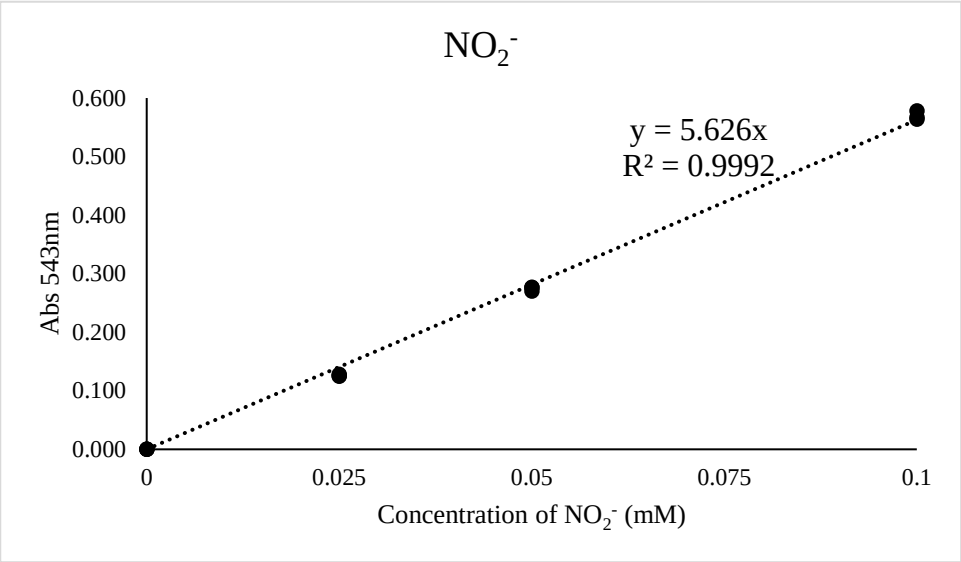

Figure A8: The standard curve made for the NO_2^- measurements. It was used to calculate NO_2^- concentrations throughout the incubation.

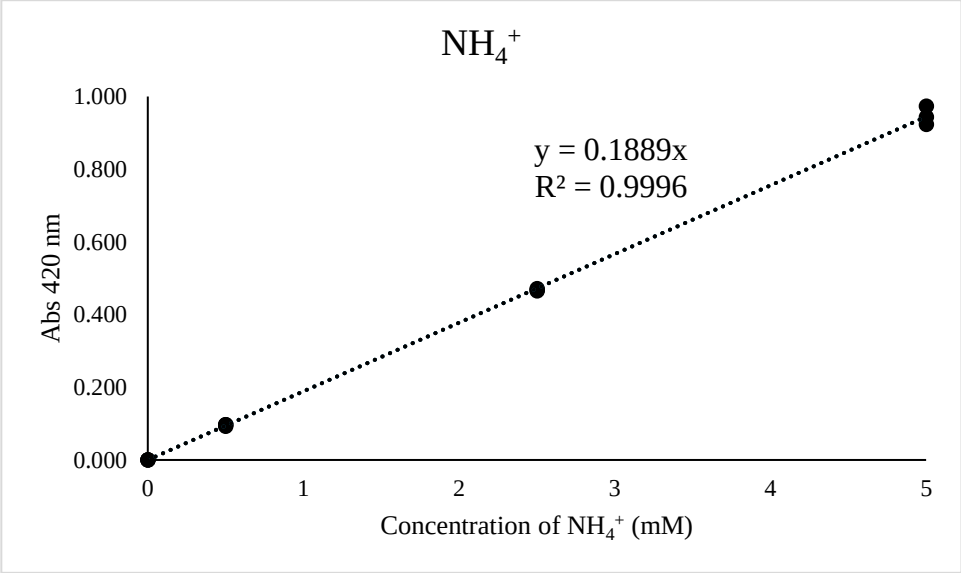

Figure A9: The standard curve for the NH_3/NH_4^+ measurements. It was used to calculate NH_3/NH_4^+ concentrations throughout the incubation.

Relative abundances of top 10 most abundant groups

To infer metabolic pathways present in the sediments, FAPROTAX analysis was performed on the amplicon data, in addition to the taxonomic analyses. Plot A10 shows the top 10 most abundant groups within each functional group.

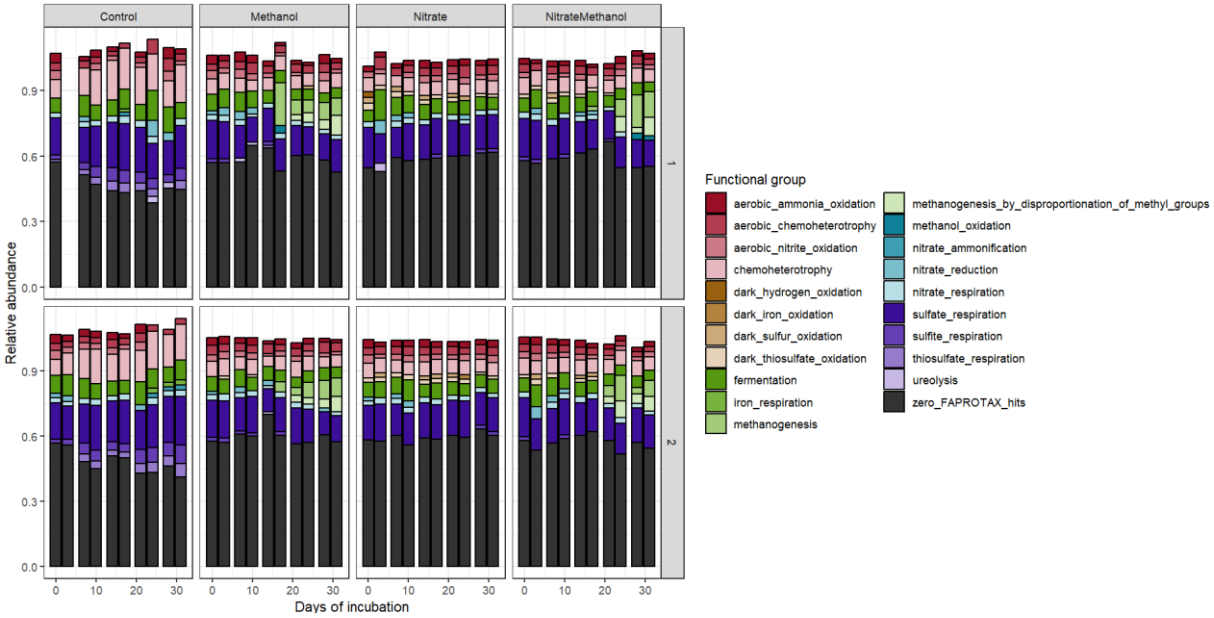

Figure A10: FAPROTAX analysis of the complete microbial composition in the samples. Approximately 60 % of all OTUs got zero FAPROTAX hits.

Primer testing

Specific *Methanolobus* primers were tested on gradient PCR to determine the optimal annealing temperature. The median temperature was set as 50 ℃ which was the Tm of the primers. The primers were tested for affinity with both *Methanolobus* DNA and Zymo mock community DNA (Zymo Research, USA) as well as a negative control. Bands formed for all temperatures with *Methanolobus* DNA. No bands was observed for the negative control. The Zymo mock community DNA (Zymo Research, USA) formed bands with the *Methanolobus* primers in the lower half of the temperature range. Since there seemed to be more specific binding in the wells with the higher temperatures the annealing temperature was chosen to be 57 ℃ (highest temperature tested).

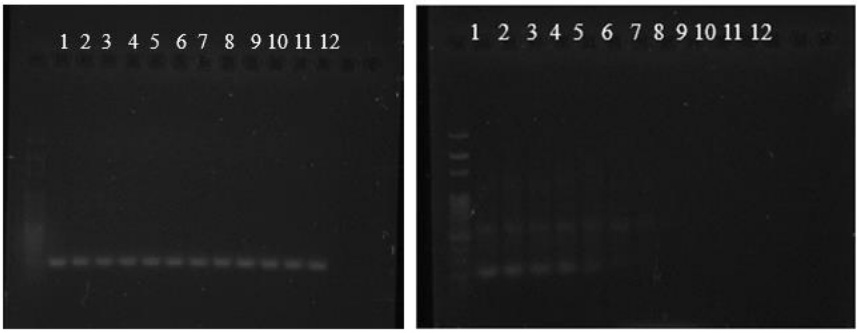

Figure A11: Visualisation of results from gel electrophoresis of the gradient PCR. Gel with *Methanolobus* DNA on the left, and Zymo mock community on the right.

Code for certain parts of the data analysis

Phyloseq and normalization

When making the Phyloseq object, filtering was performed on certain conditions:

- Only sediment samples were kept (not including the null sample)
- Samples with a total reacount less than 15000 readpairs are removed
- All domain “Eukaryota”, family “Mitochondria” and class “Chloroplast” were removed

```
readcounts <- read.delim("readcounts_vsearch_OTU.txt") %>%
        select(-c(Sample11, Sample22, Sample33, Sample44, Sample55))
        # Filtering out everything that is not a sediment sample

readcount.dta <- data.matrix(readcounts[,-1])
rownames(readcount.dta) <- readcounts$OTU

sampletable <- read.delim("metadata_KariMaster_amp_riktig.txt")
sample.dta <- data.frame(sampletable[,-3],
                         row.names=sampletable$SampleID)

sample.dta <- sample.dta %>%
  filter(n_readpairs > 15000) %>%   # Only sample02 is filtered out
  filter(Sample_type == "Sediment") %>%
  select(-c(Forward_primer, Reverse_primer, Barcode, Library_strategy,
            Library_source, Library_selection, Library_layout,
            Instrument_model, Design_description, filename, filename2,
            SequencingRunID, Rawfile_R1, Rawfile_R2, Platform))

taxonomy <- read_delim("taxonomy_vsearch_3_OTU_table.txt",
                           delim = "\t",
                           show_col_types = F) %>%
  mutate(genus = if_else(genus_score < 0.8, "Unclassified",
                         genus)) %>%
  select(-c(species, species_score))

taxon.dta <- taxonomy %>%
  select(-OTU) %>%
  as.matrix()

rownames(taxon.dta) <- taxonomy$OTU

# Making the phyloseq object
physeq.obj <- phyloseq(otu_table(readcount.dta, taxa_are_rows = T),
                       sample_data(sample.dta),
                       tax_table(taxon.dta))
physeq.obj <- physeq.obj %>%
  subset_taxa(
    domain != "Eukaryota" &
    family  != "Mitochondria" &
    class   != "Chloroplast")
```

```
# TSS normalizing the phyloseq object
TSS <- function(Xj){
  Yj <- Xj / sum(Xj)
  return(Yj)
}
physeq.tss <- transform_sample_counts(physeq.obj, TSS)

ps.tbl <- psmelt(physeq.tss)
```

Plotting figure 3.4

```
# Plotting relative abundances of taxonomic families
glom.family <- tax_glom(physeq.tss, taxrank = "family")
top.families <- names(sort(taxa_sums(glom.family),
                    decreasing=TRUE)[1:10])
prune.tbl <- prune_taxa(top.families, glom.family)
glom.tbl <- psmelt(prune.tbl)
glom.tbl %>%
  filter(Abundance != 0) %>%
  group_by(Treatment, Parallell) %>%
  arrange(desc(Abundance)) %>%
  ggplot(aes(x=Day, y=Abundance, fill=family)) +
  geom_bar(stat="identity") +
  scale_fill_manual(values= tol()) +
  facet_grid(Parallell~Treatment, scale="free") +
  theme_bw() +
  labs(y = "Relative abundance", title = "Relative abundances of families",
x = "Time (Days)")
```

Bray-Curtis PCoA by time

This PCoA analysis in R was modified from code provided by Julie Martin (PhD).

```
# Isolating the SampleIDs and OTUs from the phyloseq object
OTUs <- otu_table(physeq.tss) %>%  as.data.frame()
OTUs <- t(OTUs) # Transposing
sample_treat <- ps.tbl %>%
   select(c(Treatment, Sample, Day)) %>%
   unique()
# Merging so that treatment information is in the OTU table
OTUtbl <- OTUs %>%
  as.data.frame() %>%
  rownames_to_column(var = "Sample") %>%
  left_join(sample_treat, by = "Sample")%>%
  relocate(Treatment, .after = Sample) %>%
  relocate(Day, .after = Treatment)

fun_ord.mat <- OTUtbl %>%
  select(-c(Treatment, Day)) %>%
  column_to_rownames("Sample") %>%
  as.matrix()
fun_bray.dist <- vegdist(fun_ord.mat, method = "bray")
fun.PCoA <- cmdscale(d = fun_bray.dist, eig = TRUE)

PCo.tbl <- tibble(
  "PCo1" = fun.PCoA$points[,1], # extracting sample coordinates along PCo1
  "PCo2" = fun.PCoA$points[,2], # extracting sample coordinates along PCo2
  "Day" = OTUtbl$Day,           # including the sampling time information
  "Treatment" = OTUtbl$Treatment) %>%  # including the treatment levels
  mutate(Day = as.numeric(Day), Treatment = as.factor(Treatment))

PCoA.plt1 <- ggplot(PCo.tbl) +
  geom_point(aes(x = Day, y = PCo1, color = Treatment), size = 4) +
  geom_smooth(aes(x = Day, y = PCo1, color = Treatment),
                  method = "lm", se = FALSE) +
  labs(title = "A", x = "Time (Days)",
       y = "PCo1, 32.8 %", color = "Treatment") +
  theme(panel.background = element_blank(),
        axis.line = element_line(colour = "black")) +
  scale_color_manual(values = four_palette)

PCoA.plt2 <- ggplot(PCo.tbl) +
  geom_point(aes(x = Day, y = PCo2, color = Treatment), size = 4) +
  geom_smooth(aes(x = Day, y = PCo2, color = Treatment),
                  method = "lm", se = FALSE) +
  labs(title = "B", x = "Time (Days)",
       y = "PCo2, 15.4 %", color = "Treatment") +
  theme(panel.background = element_blank(),
        axis.line = element_line(colour = "black")) +
  scale_color_manual(values = four_palette)
```

Test over all OTUs – Control compared to methanol enrichment

Certain parts this analysis in R was modified from code provided by Julie Martin (PhD).

```
# Filtering out two treatment for the testing
test.OTUtbl <- OTUtbl %>%
   filter(Treatment == "Control" | Treatment == "Methanol") %>%
   filter(Sample != "Sample24")

wilcox.tbl <- data.frame(
  OTU = colnames(test.OTUtbl[, 3:ncol(test.OTUtbl)]),
  p_value = NA, p_adj = NA)
for (i in c(1:nrow(wilcox.tbl))) {
  w_test <- wilcox.test(test.OTUtbl[[i+2]] ~ test.OTUtbl$Treatment,
                        paired = T, exact = F)
  wilcox.tbl$p_value[i] <- w_test$p.value
}
  # adjusting the p values using fdr:
wilcox_adj.tbl <- wilcox.tbl %>%
  mutate(p_adj = p.adjust(p_value, method = "fdr")) %>%
  filter(p_adj < 0.05)

diff.tbl <- test.OTUtbl %>%
  pivot_longer(c(3:8184),
               names_to = "OTU", values_to = "Rel_abundance") %>%
  filter(OTU %in% wilcox_adj.tbl$OTU) %>%
  group_by(Treatment, OTU) %>%
  summarise(median_abundance = median(Rel_abundance)) %>%
  pivot_wider(values_from = median_abundance, names_from = Treatment) %>%
  mutate(diff_abundance = Methanol - Control) %>%
  mutate(Sign = if_else(diff_abundance > 0, 1,2))

diff.plot <- ggplot(diff.tbl, aes(x = diff_abundance,
                                  y = OTU, fill = Sign)) +
  geom_col(show.legend = F) + labs(x ="Differential abundance",title = "A")

# Taxa positively associated with methanol enrichment
pos.diff.tbl <- diff.tbl %>%
  filter(Sign == 1)

taxa <- taxonomy %>%
  filter(OTU %in% pos.diff.tbl$OTU)
# Plotting families that are positively differentially abundant
diff.plt2 <- ps.tbl %>%
  filter(OTU %in% c(taxa$OTU)) %>%
  filter(Treatment == "Methanol") %>%
  ggplot() +
  geom_line(aes(x = Day, y= Abundance),
                stat = "summary", fun = "mean", color = "blue4") +
  facet_grid(~family) +
  labs(title = "B", y = "Relative abundance", x = "Days") +
  theme_bw()
```

Norges miljø- og biovitenskapelige universitet
Noregs miljø- og biovitskapelege universitet
Norwegian University of Life Sciences

Postboks 5003
NO-1432 Ås
Norway